การโคลนและการแสดงออกของยีนที่เกี่ยวข้องกับการชีวสังเคราะห์ของลิพิดจากสาหร่ายขนาดเล็ก

นางสาวแพรไพลิน จารุจินดา

วิทยานิพนธ์นี้เป็นส่วนหนึ่งของการศึกษาตามหลักสูตรปริญญาวิทยาศาสตรมหาบัณฑิต
สาขาวิชาเทคโนโลยีชีวภาพ
คณะวิทยาศาสตร์ จุฬาลงกรณ์มหาวิทยาลัย
ปีการศึกษา 2557

CLONING AND EXPRESSION OF GENES INVOLVED IN LIPID BIOSYNTHESIS FROM MICROALGAE

Miss Pairpilin Charuchinda

A Thesis Submitted in Partial Fulfillment of the Requirements
for the Degree of Master of Science Program in Biotechnology
Faculty of Science
Chulalongkorn University
Academic Year 2014

Thesis Title	CLONING AND EXPRESSION OF GENES INVOLVED IN LIPID BIOSYNTHESIS FROM MICROALGAE
By	Miss Pairpilin Charuchinda
Field of Study	Biotechnology
Thesis Advisor	Assistant Professor Rungaroon Waditee-sirisattha, Ph.D.
Thesis Co-Advisor	Sophon Sirisattha, Ph.D.

Accepted by the Faculty of Science, Chulalongkorn University in Partial Fulfillment of the Requirements for the Master's Degree

.....Dean of the Faculty of Science
(Professor Supot Hannongbua, Dr.rer.nat.)

THESIS COMMITTEE

.....Chairman
(Associate Professor Tanapat Palaga, Ph.D.)

.....Thesis Advisor
(Assistant Professor Rungaroon Waditee-sirisattha, Ph.D.)

.....Thesis Co-Advisor
(Sophon Sirisattha, Ph.D.)

.....Examiner
(Assistant Professor Suchada chanprateep Napathorn, Ph.D.)

.....External Examiner
(Pongsaton Prapakrangkul, Ph.D.)

แพรไพลิน จารุจินดา : การโคลนและการแสดงออกของยีนที่เกี่ยวข้องกับการชีวสังเคราะห์ของลิพิดจากสาหร่ายขนาดเล็ก (CLONING AND EXPRESSION OF GENES INVOLVED IN LIPID BIOSYNTHESIS FROM MICROALGAE) อ.ที่ปรึกษาวิทยานิพนธ์หลัก: ผศ. ดร. รุ่งอรุณ วาดิถีสิริศรัทธา, อ.ที่ปรึกษาวิทยานิพนธ์ร่วม: ดร.โสภณ สิริศรัทธา, 84 หน้า.

การผลิตเชื้อเพลิงชีวภาพโดยตรงจากคาร์บอนไดออกไซด์เป็นทางออกที่ท้าทายในการแก้ไขปัญหาวิกฤตการณ์การขาดแคลนพลังงานและภาวะโลกร้อน จากการศึกษาที่ผ่านมาพบว่าสิ่งมีชีวิตขนาดเล็กที่สามารถสังเคราะห์ด้วยแสงได้ อาทิเช่น สาหร่ายขนาดเล็กและไซยาโนแบคทีเรีย เป็นแหล่งในการผลิตเชื้อเพลิงชีวภาพที่น่าสนใจ เนื่องจากมีเมแทบอลิสมที่จำเพาะต่อชีวสังเคราะห์ของลิพิด ดังนั้นเมแทบอลิสมของการสังเคราะห์ลิพิดในสาหร่ายขนาดเล็กจึงเป็นหนึ่งในเป้าหมายที่น่าสนใจเพื่อการเพิ่มประสิทธิภาพของการผลิตเชื้อเพลิงชีวภาพด้วยเทคนิคทางพันธุวิศวกรรม ในการศึกษานี้ได้ประสบความสำเร็จในการแยกยีนคาลีโอซิน (*caleosin*) ซึ่งประมวลรหัสเป็นโปรตีนบนหยดไขมัน จากสาหร่ายสีเขียว *Chlorella vulgaris* TISTR 8580 ด้วยเทคนิค RACE โดยพบว่าโปรตีนคาลีโอซินประกอบด้วย 279 กรดอะมิโน และมีมวลโมเลกุลเท่ากับ 31,047 ดาลตัน จากการศึกษาสมบัติของโปรตีนคาลีโอซินนี้ พบว่าโปรตีนคาลีโอซินไม่มีสมบัติการจับกับแคลเซียมแต่พบกิจกรรมของเอนไซม์เพอร์ออกซิจีเนส และมีสมบัติเป็นโปรตีนฮีม จากการทำ semiquantitative RT-PCR ยังพบว่ายีน *caleosin* มีการแสดงที่เพิ่มขึ้นภายใต้ภาวะความเครียดจากเกลือและภาวะขาดไนโตรเจน ในการศึกษานี้ยังได้ทำการศึกษายีนที่เกี่ยวข้องกับชีวสังเคาะห์ของกรดไขมัน โดยการโคลนและเพิ่มการแสดงออก (overexpression) ของยีนเอซิลแคริเออโปรตีนซินเทเทส (*acyl carrier protein synthetase; ACP*) ภายใต้การขับเคลื่อนของเนทีฟโปรโมเตอร์ในไซยาโนแบคทีเรีย *Synechococcus elongatus* PCC 7942 โดยยีนดังกล่าวจะประมวลรหัสเป็นเอนไซม์เอซิลแคริเออโปรตีนซินเทเทส (acyl carrier protein synthetase) จากการวิเคราะห์และเปรียบเทียบกรดไขมันภายในเซลล์แสดงออกเกินกับเซลล์ชุดควบคุมพบว่า เซลล์แสดงออกเกินและเซลล์ชุดควบคุมมีการสังเคราะห์กรดไขมันปาล์มิติกและปาล์มิโตเลอิกเป็นกรดไขมันหลัก นอกจากนี้ยังพบว่าในเซลล์แสดงออกมีปริมาณกรดไขมันรวมสูงกว่าเซลล์ชุดควบคุมประมาณ 3.7 เท่า ภายใต้ภาวะการเจริญปกติ แต่ไม่พบความแตกต่างดังกล่าวในภาวะการเจริญที่มีความเครียด ดังนั้นการพัฒนาสายพันธุ์ด้วยเทคนิควิศวกรรมเมแทบอลิกด้วยยีนคาลีโอซินและเอซีพีอาจเป็นวิธีการที่ดีในการเพิ่มการผลิตเชื้อเพลิงชีวภาพในสาหร่ายขนาดเล็กต่อไป

สาขาวิชา เทคโนโลยีชีวภาพ ลายมือชื่อนิสิต .....

ปีการศึกษา 2557 ลายมือชื่อ อ.ที่ปรึกษาหลัก .....

ลายมือชื่อ อ.ที่ปรึกษาร่วม .....

5572210123 : MAJOR BIOTECHNOLOGY

KEYWORDS: LIPID BIOSYNTHESIS / MICROALGAE / ACYL CARRIER PROTEIN SYNTHETASE / CALEOSIN / LIPID DROPLET

PAIRPILIN CHARUCHINDA: CLONING AND EXPRESSION OF GENES INVOLVED IN LIPID BIOSYNTHESIS FROM MICROALGAE. ADVISOR: ASST. PROF. RUNGAROON WADITEE-SIRISATTHA, Ph.D., CO-ADVISOR: SOPHON SIRISATTHA, Ph.D., 84 pp.

Production of biofuel directly from CO_2 is a challenging approach to solve the near world energy shortage and environmental problems. Accumulating evidence showed that photosynthetic microorganisms would serve as attractive sources because of several unique metabolisms for lipid biosynthesis. Microalgal lipid metabolism is one of the attractive targets to enhance their efficiency in biofuel production by genetic engineering. In the study, *caleosin* gene encoding lipid droplet protein was successfully isolated from green alga *Chlorella vulgaris* TISTR 8580 by RACE-method. The deduced polypeptide comprises of 279 amino acid residues with a molecular mass of 31,047 dalton. *Chlorella* caleosin was expressed and functionally analyzed. It was shown that *Chlorella* caleosin had no calcium binding property but it had peroxygenase activity. It was found to be a hemoprotein. Semiquantitative RT-PCR revealed that *caleosin* gene was up-regulated under salt stress and nitrogen deficiency. Furthermore, gene involved in fatty acid biosynthesis was also performed. *Acyl Carrier Protein synthetase* (*ACP*) gene from fresh water cyanobacterium *Synechococcus elongatus* PCC 7942 was cloned and overexpressed under native promoter. Intracellular fatty acid profiles in mock control and overexpressing cells were compared. Palmitic and palmitoleic acids were major fatty acids. Interestingly, total fatty acid of the overexpressing strain was higher than the control approximately 3.7-fold under normal condition but no difference under stress condition was observed. Therefore, metabolic engineering of *caleosin* or *ACP* has potential to further enhance biofuel production in microalgae.

Field of Study: Biotechnology
Academic Year: 2014

Student's Signature .....
Advisor's Signature .....
Co-Advisor's Signature .....

ACKNOWLEDGEMENTS

I would like to express my sincere gratitude and deep appreciation to my advisor and my co-advisor, Assistant Professor Dr. Rungaroon Waditee Sirisattha and Dr. Sophon Sirisattha for their excellent instruction, guidance, encouragement, and supported throughout the course of my research. In addition, I would also like to express my thanks to thesis committee, Associate Professor Dr. Tanapat Palaga, Assistant Professor Dr. Suchada Chanprateep Napathorn and Dr. Pongsaton Phapugrangkul for their comments and valuable suggestions in this research. My appreciation is also expressed to Professor Dr. Teruhiro Takabe, Professor Dr. Yoshito Tanaka and Associate Professor Dr. Hakuto Kageyama for their help in laboratory and suggestion during my stay in Japan. I would like to gratefully acknowledge the fund supported of CU. graduate school thesis grant from Chulalongkorn University, Thailand. Special thanks for all my special friends and members of laboratory room 1904/17 for encouragement and nice friendships. Finally, I would like to express my thanks to my family for their warmest love, care, encouragement, understanding, support and attention throughout my life.

CONTENTS

Page

Page

Page

LIST OF TABLE

LIST OF FIGURES

LIST OF ABBREVIATIONS

A	Absorbance
Bp	Base pair
BSA	Bovine serum albumin
°C	Degree Celsius
Kb	Kilo base pair
kDa	Kilodalton
g	Gram
µg	Microgram
hr	Hour
l	Liter
mA	Milliampare
min	Minute
µl	Microliter
ml	Milliliter
mM	Milli Molar
M	Molar
nm	Nanometer
RACE	Rapid amplification of cDNA end
PCR	Polymerase chain reaction
rpm	Revolution per minute
CH_3COONa	Sodium acetate
NaCl	Sodium chloride
$NaNO_3$	Sodium nitrate
SDS	Sodium dodecyl sulphate
UV	Ultraviolet
W/m^{-2}	Watts per square meter

CHAPTER I

INTRODUCTION

In the past decade, the demand of sustainable energy becomes one of the most concerns because of the world energy crisis (Huang *et al.*, 2010). The global primary energy demand is estimated by Energy Information Administration (EIA) in 2012 (the U.S. Energy Information Administration (EIA), 2012). It will practically redouble in 2030 when compared with the demand in 1990 because of a growth of world population and the economy. As expected, India and China, the new developing economic countries will consume a lot of global energy and cause to more environmental damages (Mata *et al.*, 2010). The forecast of world energy consumption, available petroleum fuel consumption is assumed that it will be declined by 80% in 2050. Due to that decreasing, the petroleum fuel cost is expected to increase correspondingly (Stephens *et al.*, 2010). Therefore, sustainable energy should be developed to solve the near energy shortage crisis. There are many problems in both petroleum fuel production and consumption such as limitation sources and unstable cost. Moreover, petroleum fuel production can release high level of CO_2 that is not environmentally friendly (Radakovits *et al.*, 2010). For example, the transportation and energy sectors are the major greenhouse gas emissions sources in European Union. Greenhouse gas can affect both global warming and other environmental impact such as acidification of sea water (Mata *et al.*, 2010). Thereby, sustainable energy study is highly challengeable. There are numerous kinds of sustainable energy sources. Some natural energy sources can be developed as sustainable energy (*i.e.* wind, water, geothermal, and solar) (La Russa *et al.*, 2012). Although solar energy is abundant and surplus for global energy demand, this kind of energy is dispersed and difficult to apply. Consequently, photosynthetic organisms are interesting because of their potential for solar energy collecting and converting into organic molecules (Schenk *et al.*, 2008, La Russa *et al.*, 2012).

Biofuel is a well-known sustainable energy that is derived from a living or living organisms. It is an attractive sustainable energy due to it is a storage form of

solar energy. In addition, it can be used directly in existing engines for transportation (Scott *et al.*, 2010). In first generation biofuel, plant biomass has been intensively focused for biofuel production such as bioethanol, biodiesel, and biomethane (Schenk *et al.*, 2008). Various types of crops such as sugar cane, sugar beet, and corn starch were used as biofuel resources. These crops can be converted into bioethanol by fermentation. Moreover, oil crops such as palm and grape seed oil were used in biodiesel production (Hill *et al.*, 2006, Scott *et al.*, 2010, Stephens *et al.*, 2010). However, crop plants are not the ideal resources for biofuel production because of many mentions. For instance, plant growing needs arable land which is limited on the earth's surface area (Hu *et al.*, 2008). Furthermore, the requirement of crop plants is directly competitive to human food and animal feed (La Russa *et al.*, 2012, Liu *et al.*, 2013). For the next generation biofuel, other photosynthetic organisms are realized. Microalgae are oxygenic photosynthetic microorganisms that have several unique metabolisms. They offer several advantages in biofuel production such as high photosynthetic efficiency, high growth rate or high biomass yield, ability to grow on non-arable land and their ability to produce energy-rich compounds as potential biofuel precursors (Hu *et al.*, 2008, Radakovits *et al.*, 2010, La Russa *et al.*, 2012). Although, they can be resources in biofuel production, ability in lipid production of wild-type strains remains limited. Lipid biosynthesis is one of attractive targets for strain improvement to enhance the efficiency in biofuel production by genetic engineering.

In general, microalgal lipid biosynthesis metabolisms are categorized into three major parts. These are lipid droplet (LD) formation, fatty acid synthesis, and hydrocarbon synthesis. Nowadays, many researches have been carried out to understand lipid biosynthesis metabolism in microalgae. For LD formation, some microalgae have the ability to accumulate LDs under extreme conditions such as nitrogen deficiency and high light condition (Liu *et al.*, 2013). LD formations could be induced in *Chlorella* sp. (Lin *et al.*, 2012) and also *Auxenochlorella protothecoides* (Pasaribu *et al.*, 2014) under nitrogen deprivation. Accumulating evidence has been shown that caleosin was a major lipid droplet protein in microalgal LD (Nguyen *et al.*,

2008, Peled *et al.*, 2011). Although, microalgal LD proteins have been reported, little is known about their physiological functions.

Fatty acid biosynthesis comprises a complex set of genes. Acyl carrier protein (ACP) is one of attractive target for genetic manipulation as it is believed to be involved in elongation of lipid. Acyl-acyl carrier protein synthetase gene (*aas*) was isolated and identified from cyanobacteria *Synechocystis* sp. PCC 6803 and *Synechococcus elongatus* PCC 7942 (hereafter *S. elongatus* PCC 7942) (Kaczmarzyk & Fulda, 2010). Loss-of-function of AAS in these cyanobacteria reduced ability of exogenous fatty acids utilization. These results suggested that AAS is involved in the recycling of exogenous fatty acids (Kaczmarzyk & Fulda, 2010). Ruffing and Jones reported the engineered *S. elongatus* PCC 7942 using *ACP* and thioesterase (*tesA*) genes. The expressing cells could produce and secret free fatty acids in a small-scale production (Ruffing & Jones, 2012). For hydrocarbon synthesis in microalgae, they mostly focused on alkane production. There are two enzymes involved in alkane biosynthesis pathway, namely acyl–acyl carrier protein reductase and aldehyde decarbonylase. As heterologous expression, alkane biosynthesis genes from *S. elongatus* PCC7942 could support the ability of hydrocarbon production and secretion in *Escherichia coli* expressing cells (hereafter *E. coli*) (Schirmer *et al.*, 2010). The biosynthesis hydrocarbon waxes also have been carried out. A long-chain acyl-CoA reductase (ACR) from *S. elongatus* PCC7942 was overexpressed in *E. coli*. Functional analysis revealed ACR is actually reductase enzyme which catalyzes fatty acyl-CoA esters to corresponding aldehydes with NADPH dependency (Lin *et al.*, 2013).

In this study, I aimed to clone and express genes involved in lipid biosynthesis from microalgae. There are two target genes; (1) putative *caleosin* gene from green alga *Chlorella vulgaris* TISTR 8580 (hereafter *C. vulgaris* TISTR 8580), and (2) putative *acyl carrier protein synthetase (ACP)* gene from cyanobacterium *S. elongatus* PCC 7942 (synpcc7942_0918).

The objective of this research:

1. To clone *caleosin* gene from *C. vulgaris* TISTR 8580 and *ACP* gene from *S. elongatus* PCC 7942.

2. To express the cloned *caleosin* gene in *E. coli* and functionally characterize.

3. To overexpress *ACP* gene in *S. elongatus* PCC 7942 and monitor lipid profile in expressing cells.

CHAPTER II
LITERATURE REVIEW

2.1 Biofuel production

Biofuel is broadly defined as a fuel (*i.e.* solid, liquid, or gas) which consists of biological material derived from living, or recently living organisms (Patil *et al.*, 2008). Biofuel production was intensively discussed due to its requisite for environmental and economic sustainability. First generation biofuel refers to the production from food crops such as grains, sugar beet, sugar cane, corn, and oil seeds (Scott *et al.*, 2010). However, food crops were not the most suitable source to replace fossil fuel because they competed with agricultural and farm products for human foods and animal feeds. Then, second generation biofuel has been studied. In this generation, biofuel is produced from non-food feed stocks (e.g. woods, leaves, and agricultural residues) through fermentation. For example, bioethanol was produced from lignocellulose (Scott *et al.*, 2010). Nevertheless, conversion of non-food biomass into the fermentable form requires costly enzymatic pre-treatment process (Fernandes *et al.*, 2010). Consequently, production of biofuel from photosynthesis microorganisms (microalgae and cyanobacteria) recognize as third generation. To date, microalgae offer great potential as feed stocks for biofuels. Microalgae are photosynthetic microorganisms which comprise of both prokaryotes (e.g. cyanobacteria) and eukaryotes (e.g. green algae and diatoms) (Li, 2008). Microalgal habitats are extremely diverse, ranging from freshwater, marine, brackish, and other extreme conditions (Hu *et al.*, 2008). Microalgae have been studied to produce many kinds of biofuels which comprise of biodiesel, bio-oil, bio-syngas, and bio-hydrogen (Li, 2008). There are several attractive advantages in production as follows (Hu *et al.*, 2008, Li, 2008, Radakovits *et al.*, 2010, Scott *et al.*, 2010, Liu *et al.*, 2013).

1. They synthesize and accumulate large quantities of neutral lipids (approx. 20–50% of cell dry weight). In some microalgal strain, *Botryococcus braunii*

accumulates high amount of lipid approximately 60 % of cell dry weight (Metzger & Largeau, 2005).

2. They have high growth rates (*i.e.* 1–3 doublings per day). Thus, their biomasses will be possible to satisfy the energy demand using limited land for cultivation.

3. They are able to grow in diverse habitats such as saline, brackish water, and coastal seawater which are not suitable for commercial agriculture.

4. They use some nutrients such as nitrogen and phosphorus for growing from the waste water sources. Thus, they also provide a bio-remediation benefit in waste water treatment.

5. They utilize carbon dioxide (CO_2) which is a major of greenhouse gas (GHG) as a carbon source. From this fact, GHG accumulation can be reduced, thus slow down global warming crisis.

6. They produce high value co- or by- products. These are vegetable oil, essential fatty acids, biopolymers, proteins, polysaccharides, pigments, animal feeds, fertilizers, and hydrogen gas (H_2).

7. Their growths are suitable to culture either in photo-bioreactors or skyscrapers that can enhance biomass yields and save arable land.

8. Their cultivation consumes less water than conventional land crops.

Currently, microalgal biofuels are still not suitable to use as an economically viable biofuel feed stock in reality due to their very high production cost. Therefore, attractive strain improvements and low-energy strategies are needed to overcome those problems.

2.2 Microalgal metabolic pathways

The ability to produce a wide variety of biofuels in microalgae has been investigated (Li, 2008). Due to the fact that microalgae have diverse metabolisms (Figure 1), microalgae can produce and accumulate a variety of energy storage compounds such as lipids (*i.e.* triacylglycerol (TAG)), alcohols, hydrocarbons, polysaccharides, and other energy-rich compounds which are possible to utilize as potential biofuel feed stocks (Radakovits *et al.*, 2010). Their metabolic pathways can be modified through genetic engineering to develope of biofuel production efficiency.

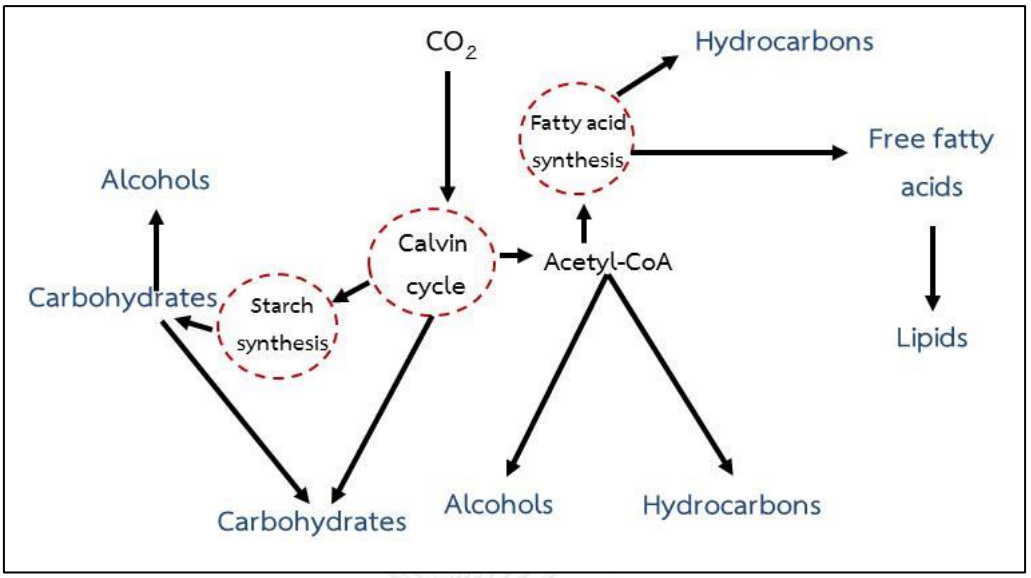

Figure 1: Microalgal lipid metabolism related pathways (modified from; Radakovits et al., 2010).

2.2.1 Lipid biosynthesis in microalgae

In these photosynthesis organisms, lipid biosynthesis involved in two major parts; free fatty acid synthesis and TAG assembly together with LD formation (Radakovits *et al.*, 2010). LD formation has been found in eukaryotic microalgae only (Liu *et al.*, 2013). The simplified overview of microalgal lipid biosynthesis is shown in Figure 2. Firstly, free fatty acids are synthesized in the chloroplast. Then, they are assembled with glycerol backbone as well as TAGs formation at endoplasmic reticulum (ER).

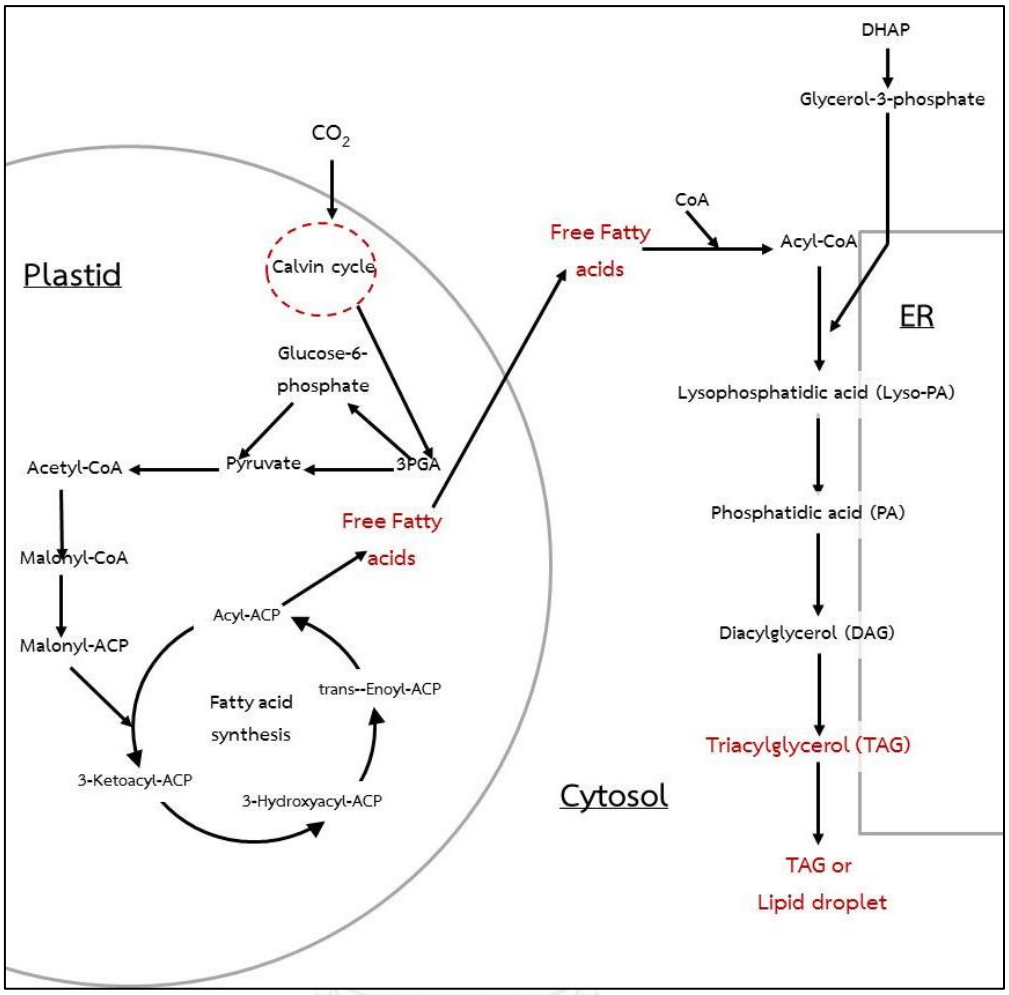

Figure 2: Simplified overview of lipid biosynthesis pathway in eukaryotic microalgae (modified from; Radakovits *et al*., 2010). Acyl carrier protein (ACP), dihydroxyacetone phosphate (DHAP), endoplasmic reticulum (ER), 3-phosphoglyceric acid (3PGA), and triacylglycerol (TAG).

2.2.1.1 Fatty acid biosynthesis

A generalized scheme for fatty acid biosynthesis in microalgae is shown in Figure 3. Initially, acetyl-CoA is converted into malonyl-CoA by acetyl-CoA carboxylase (ACCase) (1). Then, malonyl CoA:ACP transferase further transfers malonyl group from CoA to acyl carrier protein (ACP) to form malonyl ACP (2). Malonyl ACP is the carbon donor for subsequent elongation reactions by condensation reaction (3). After subsequent condensations, 3-ketoacyl ACP will be

reduced by 3-ketoacyl ACP reductase (4). Next, the reducing product is dehydrated (5) and reduced again (6) by 3-hydroxyacyl ACP dehydrase and enoyl ACP reductase, respectively. Taken together, this pathway generates either C16 or C18 fatty acids (acyl-ACP forms) which are the precursors of membrane and TAG formation (Hu *et al.*, 2008).

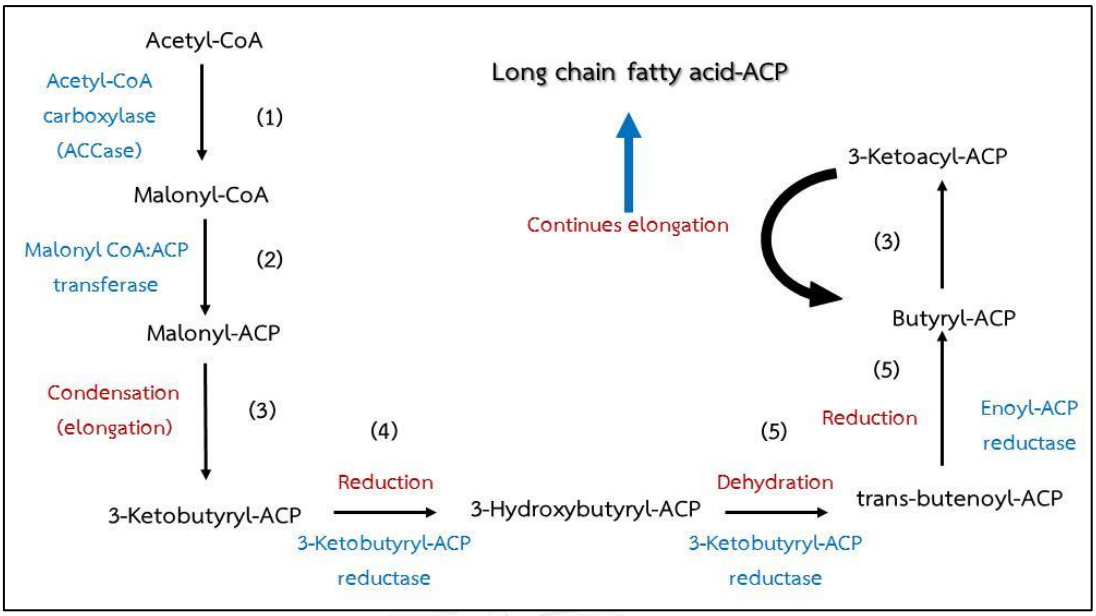

Figure 3: The de novo synthesis of fatty acids in microalgae (modified from; Hu *et al.*, 2008). Blue represents enzyme names and red represents chemical reactions, respectively.

As above description, ACP offers an important role in fatty acid elongation as well as a protein co-factor. All subsequent reactions in fatty acid biosynthesis associated with ACP until their products are successfully produced. Present research aims to study ACP synthesis gene (*ACP synthetase*) due to expectation that exceeding ACP may support and/or modulate fatty acid synthesis in the expressing or overexpressing cells.

2.2.1.2 TAG biosynthesis

TAG is a major storage form of neutral lipid in microalgae (Radakovits *et al.*, 2010). It is an important composition in LD as a main neutral lipid in its core structure. As shown in Figure 4, TAG is synthesized through glycerol pathway in ER. Fatty acids from chloroplasts are sequentially transferred from CoA to positions 1 and 2 of glycerol-3-phosphate (G-3-P) to form lyso-phosphatidic acid (Lyso-PA) and

phosphatidic acid (PA) by cytosolic glycerol-3-phosphate acyl transferase (1) and lyso-phosphatidic acid acyl transferase (2), respectively. Then, PA is dephosphorylated by phosphatidic acid phosphatase (3) resulting in diacylglycerol (DAG) production. Finally, the last fatty acid is transferred to position 3 of DAG by diacylglycerol acyltransferase (DAGAT or DGAT) to yield TAG (Hu *et al.*, 2008).

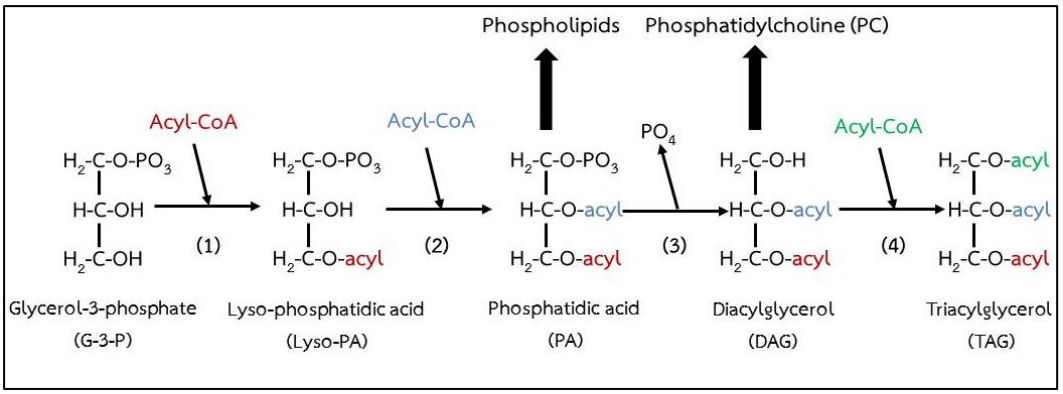

Figure 4: TAG biosynthesis pathway in microalgae (modified from; Hu *et al*., 2008).

2.2.1.3 Lipid droplet protein (LD)

LD can be referred to oil droplet, lipid body or oil globule. In microalgae, these storage organelles reserve carbon and energy sources in cells. Localization of microalgae LDs has been found in both cytoplasm and chloroplast similar as found in plants (Liu *et al.*, 2013). In addition of the function as storage organelles in higher plants, LDs are involved in other aspects, including stress response, hormone signaling, and plant development (Liu *et al.*, 2013). LDs mainly compose of neutral lipids, mainly TAGs in their core. They are surrounded by monolayer of phospholipids embedding with some integral proteins. In higher plants, three kinds of LDs have been reported. These are oleosin, caleosin, and stereosin (sterol dehydrogenase) (Chapman *et al.*, 2012). However, caleosin is only LD, reporting in microalgae and fungi. Plant caleosins and oleosins are calcium binding proteins. A model of plant caleosin is shown in Figure 5. Its structure has a long hydrophobic hairpin part with proline knot motif. N-terminal region contains EF-hand motif, responsible for calcium binding site. There are many conserved protein phosphorylation sites on C-terminal region. Both N-terminal and C-terminal regions expose to cytosol. They have conserved histidine residues for heme prosthetic group binding (Chapman *et al.*, 2012).

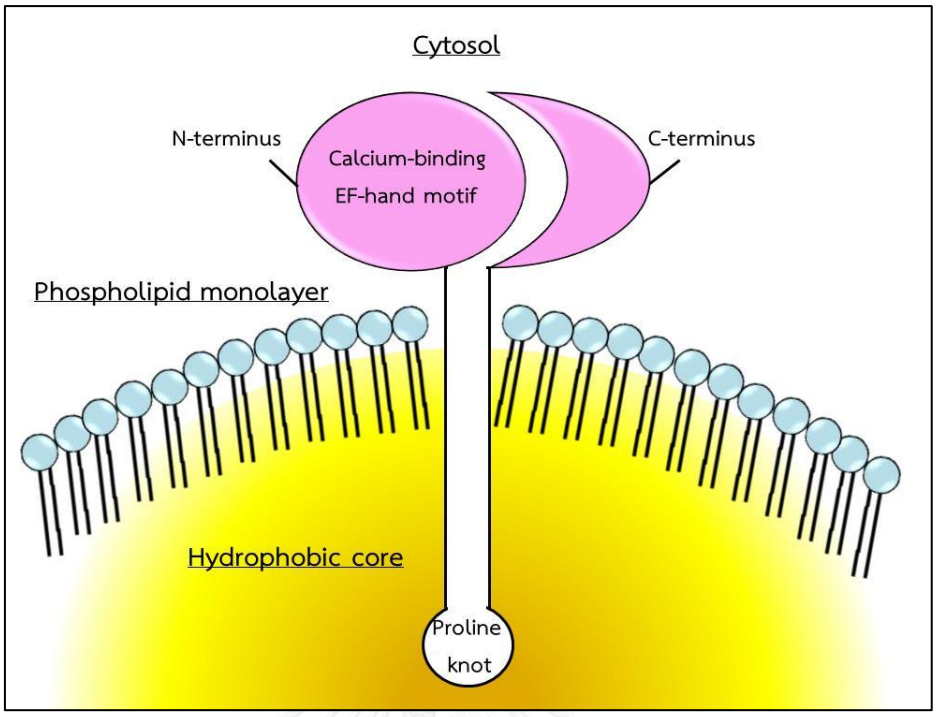

Figure 5: Schematic structure of plant caleosin protein (modified from; Chapman *et al*., 2012).

According to the structure, plant caleosin has several functions such as hemo-protein because of their histidine residues, peroxygenase that involves in lipid transformation by epoxidation reaction (Hanano *et al.*, 2006, Chapman *et al.*, 2012). They are also calcium binding proteins (Hanano *et al.*, 2006). For microalgae, the *Chlorella* LD could be induced by nitrogen limitation (Lin *et al.*, 2012). *Chlorella* LD is less stable than plant LD that shows during membrane fractionation. Stable *Chlorella* LD is comprised of lipid droplet surface protein, namely caleosin (Lin *et al.*, 2012). In *Auxenochlorella protothecoides*, nutrient limitation could induce LD formation and further affected to their fatty acid profile. *Auxenochlorella* caleosin was found and localized at lipid droplet membrane when characterized by immunolocalization assay. Moreover, *caleosin* gene was up-regulated in this microalga under nutrient limitation condition (Pasaribu *et al.*, 2014). Though, the studies of microalgal caleosin have been reported, little is known about their functions. Therefore, this research aims to isolate, express, and functionally characterize of caleosin from microalgae.

2.2.2 Hydrocarbon biosynthesis in microalgae

Hydrocarbon biosynthesis, particularly for alkane, has been investigated in cyanobacteria model (Schirmer *et al.*, 2010). Two enzymes involved in alkane biosynthesis such as acyl–ACP reductase (AAR) and an aldehyde decarbonylase (ADO) have been reported. The intermediates from fatty acid metabolism will be changed to hydrocarbon compounds by catalysis of those enzymes. As shown in Figure 6, fatty acyl-ACP is firstly converted into fatty aldehyde by AAR (1). Then, ADO will catalyze fatty aldehyde product into the corresponding alkane or alkene (2).

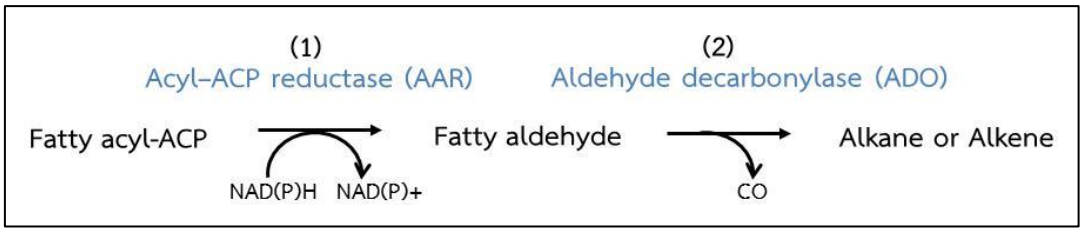

Figure 6: Alkane biosynthesis pathway in cyanobacteria.

In this study, I aimed to clone and express genes involved in lipid biosynthesis from microalgae. There are two target genes; (1) putative *caleosin* gene from green alga *Chlorella vulgaris* TISTR 8580 (hereafter *C. vulgaris* TISTR 8580), and (2) putative *acyl carrier protein synthetase (ACP)* gene from cyanobacterium *S. elongatus* PCC 7942 (accession number: synpcc7942_0918). In this study, I have three objectives as follows.

The objective of this research:

1. To clone *caleosin* gene from *C. vulgaris* TISTR 8580 and *ACP* gene from *S. elongatus* PCC 7942.
2. To express the cloned *caleosin* gene in *E. coli* and functionally characterize.
3. To overexpress *ACP* gene in *S. elongatus* PCC 7942 and monitor lipid profile in expressing cells.

CHAPTER III

MATERIALS AND METHODS

Materials

3.1 Instruments

Affinity chromatography column: Hitrap FF column, GE Healthcare Life Sciences, USA

Autoclave: Model HA 30, Hirayama Manufacturing Cooperation, Japan

Autopipette: Pipetteman, Gilson, France

Chromatography system: Model AKTA prime GE Healthcare Life Sciences, USA

Electrophoresis unit: Model mini protein II cell: Biorad, USA

Freeze dryer: Flexi-Dry MP, Kinetics, USA

Gas chromatography: Agilent 6890N network GC, Agilent technologies, USA

Gel imaging: Model Gel Doc EZ Imager, Biorad, USA

Illuminated/Refrigerated orbital: Sanyo, England

Incubator: Haraeus, Germany

Incubator shaker: Psyco-therm, New Bruncwick Scientific Supply, USA

INSONATOR 201M: Kubota, Japan

Laminar flow BVT-124: International Scientific Supply, Thailand

Microcentrifuge: Kubota, Japan

NanoDrop 2000 UV-Vis Spectrophotometer: Thermo scientific, USA

pH meter: PHM 83 Autocal pH meter, Radiometer, Denmark

Power supply: Pharmacia, England

Refrigerated centrifuge: Model J-21C, Beckman Instrument Inc, USA

Spectrophotometer UV-240: Shimadzu, Japan

Vacuum dry: Taitech, Japan

Vortex: Model K-550-GE: Scientific Industries, USA

3.2 Chemicals

Acrylamide: Merck, USA

Ammonium persulfate: Katayama Chem, Japan

An antibody raised against 6-histidine: R&D systems, USA

An antibody raised against mouse: Biolab, England

Ampicillin: Katayama Chem, Japan

Bacto tryptone: Merck Ag Darmstadt, Germany

Bacto Yeast extract: Merck Ag Darmstadt, Germany

Butylated hydroxytoluene: Sigma, USA

Calcium chloride: Merck Ag Darmstadt, Germany

Chloroform: Katayama Chem, Japan

Coomasie brilliant blue R-250: Sigma, USA

Ethanol: Katayama Chem, Japan

Fatty acids standard: Sigma, USA

Glycerol: Merck Ag Dramstadt, Germany

Hexane: Sigma, USA

Hydrochloric: Sigma, USA

Isopropyl β-D-1-thiogalactopyranoside: Sigma, USA

Magnesium chloride: Merck Ag Dramstadt, Germany

Magnesium sulfate: Merck Ag Dramstadt, Germany

Nile red solution: Sigma, USA

Phenol: Katayama Chem, Japan

Potassium chloride: Merck Ag Dramstadt, Germany

SYBR safe DNA gel stain: Life technologies, USA

Sodium acetate: Sigma, USA

Sodium chloride: Sigma, USA

Sodium nitrate: Sigma, USA

Sodium sulfate: Sigma, USA

Streptomycin: Sigma, USA

3.3 Membranes

PVDF/Nitrocellulose membrane: Millipore Cooperation, USA

3.4 Kits

Amicon Ultra-2: Sigma, USA

DNeasy Plant mini kit: Qiagen, Germany

Gel extraction kit: Invitrogen, USA

HRP conjugate substrate kit: Biolab, USA

PureLink Quick Plasmid Miniprep kit: Invitrogen, USA

RNeasy Plant Mini Kit: Qiagen, Germany

Standard molecular weight: Biorad, USA

3.5 Enzymes and restriction enzymes

Reverse transcription enzyme M-MLV: Takara, Japan

*Bam*HI: Biolabs, USA

*Xho*I: Biolabs, USA

3.6 Bacterial, microalgal strains and plasmids

Table 1: Bacterial, microalgal strains and plasmids used in this study

Strains and plasmids	Description	Source/reference
C. vulgaris TISTR 8580	Fresh water green alga	Thailand Institute of Scientific and Technological Research (TISTR), Thailand
E. coli DH5α	*sup*E44 Δ*lac*U169 (φ80 *lacZ* ΔM15) *hsd*R17 *recA1 endA1 gyrA96 thi*-l *rel*A1	Invitrogen, USA
E. coli BL21	(B F– *dcm omp*T *hsd*S (rB-mB-) *gal* [malB+] K-12 (λS)	Invitrogen, USA

E. coli BL21(DE3)	(F–*omp*T *gal dcm lon hsd*SB (rB- mB-) λ (DE3 [lac1 *lac*UV5-T7 gene 1 *ind*1 *sam*7 *nin*5])	Invitrogen, USA
S. elongatus PCC 7942	Fresh water cyanobacterium	Research Institute of Meijo University, Japan
Caleosin/pCold I	837 bp *Caleosin* fragment cloned into pCold I	This study
ACP7942/pUC303	2.3 kb *ACP7942* fragment together with its promoter cloned into pUC303	This study
pGEM-T Easy	TA-cloning vector	Promega, USA
pMD20	TA-cloning vector	Takara, Japan
pUC303	Expressing shuttle vector	Nomura *et al*., 1995

Methods

3.7 Expression and functional analysis of *caleosin* gene from *C. vulgaris* TISTR 8580

3.7.1 Strains and growth conditions

3.7.1.1 *E. coli* culture condition

E. coli strain DH5α, BL21, and BL21 (DE3) cells were grown in Luria-Bertani (LB) medium (Appendix 1) at 37°C and were used as general purpose on cloning and expression. *E. coli* transformed cells were grown under the same

conditions as wild-type cells but were supplemented with appropriate antibiotics. The growth of bacterial cells was monitored by measuring the absorbance at 620 nm with a Shimadzu UV-160A spectrophotometer (Shimadzu, Japan).

3.7.1.2 *C. vulgaris* TISTR 8580 culture condition

Fresh water green alga, *C. vulgaris* TISTR 8580 cells were grown photoautotrophically (120 μE m^{-2} s^{-1}) in BlueGreen (BG) 11 liquid medium (Appendix 2) with shaking 150 rpm at 30°C (Rippka *et al.*, 1979). The growth of algal cells was monitored by measuring the absorbance at 730 nm with a Shimadzu UV-160A spectrophotometer (Shimadzu, Japan).

For physiological and stress experiments, *C. vulgaris* TISTR 8580 cells were grown photoautotrophically (120 μE m^{-2} s^{-1}) with shaking 150 rpm at 30°C as normally cultural condition (from 3.7.2.2) until the absorbance at 730 nm (A730) reached 0.4 prior to other culture conditions. There were three different stress media to further grow *C. vulgaris* TISTR 8580 cells for in vivo experiments according to the difference of BG11 media composition as follows.

A. Sodium nitrate depletion (hereafter nitrogen deficiency): all sodium nitrate (18 mM $NaNO_3$) was removed from BG11 medium,

B. BG11 with 0.3 M NaCl (hereafter salt stress): BG11 medium was supplemented with 0.3 M NaCl,

C. BG11 with 50 mM CH_3COONa (hereafter sodium acetate stress): BG11 medium was supplemented with 50 mM CH_3COONa.

For stress condition, one hundred milliliters of algal cells which A730 reached 0.4 under normal culture were harvested by centrifugation at 8,000 rpm for 10 min. Then, harvested cells were washed at least three times by new liquid media and transferred to each stress condition (A, B, and C).

3.7.2 Isolation of *caleosin* from *C. vulgaris* TISTR 8580

Partial sequence of ***c****aleosin* gene from *C. vulgaris* TISTR 8580 was hunted by using degenerated primers (ACMKSACGGTSMTGCAGCAGCA, Clom-F, and TTYT CSGGSACAAARCGVCCCTC, Clom-R). PCR products were cloned into pCR2.1 and sequenced (kindly performed and obtained sequences by Research Institute of Meijo University, Japan). Nucleotide sequence that showed high homology to caleosin gene was further used to design new primer set. The full length cDNA was obtained by RACE-method using the primer set: ACCGCGACAACGACGGTGTGCTG, CvClo-F3, and CCAGGAGAAGG TGCCGTGGATGAC, CvClo-R5.

To construct *Chlorella caleosin* in expression vector pCold I, the coding region were amplified by PCR using the specific primers, ACATATGG TGTCGGCTTCCCAGATG, CvClo-F, and AGAATTCTCACTCCTCCTTGGCCCC TGCC, CvClo-R. This primer set was designed to introduce *Nde*I and *EcoR*I restriction sites on the 5' and 3' end of PCR products, respectively. The PCR products were cloned into pCR2.1 vector and sequenced to exclude PCR errors. The full-length *caleosin* fragment size approximately 1.3 kb was prepared by double digestion with *Nde*I and *EcoR*I and ligated into the corresponding sites of pCold I. The recombinant plasmid, c*aleosin* fragment cloned into pCold I (hereafter *caleosin*/pCold I) was firstly transformed into *E. coli* DH5**α** cells for propagation. Then, it was transformed into *E. coli* strain BL21 for expression. Schematic of construction was simply illustrated in Figure 7.

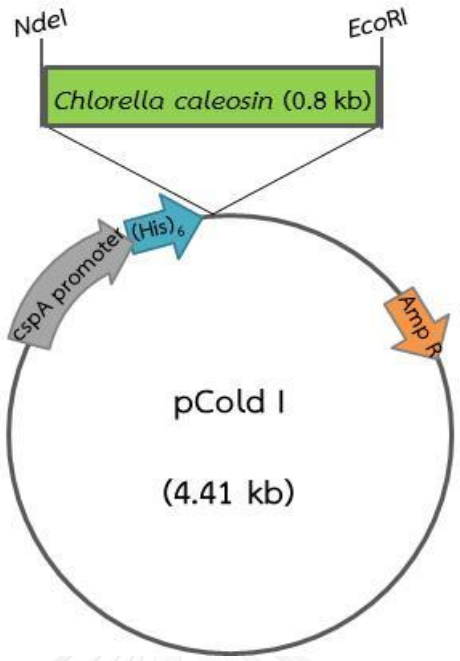

Figure 7: Contruction of the *caleosin* from *C. vulgaris* TISTR 8580 in pCold I. CspA promoter: cold-inducible promoter; (His)6: 6-histidine; Amp R: ampicillin resistant gene.

3.7.3 Bioinformatics analysis

A sequence of *Chlorella* caleosin (obtained from this study) was compared with several available caleosin protein sequences from various organisms (*i.e.* fungi, green algae, and plants). These representative caleosin protein sequences retrieved from UniProt and NCBI databases. Sixteen caleosin sequences are obtained from fungi (*Magnaporthe oryzae* 70-15; accession number XP_365887, *Neurospora crassa*; accession number Q7S2T2, and *Ustilago maydis*; accession number Q4PAW0), green algae (*Auxenochlorella* protothecoides; accession number AEB77763, *Coccomyxa subellipsoidea* C-169; accession number EIE19761.1 and EIE19762.1, and *Volvox carteri*; accession number XP_002958325.1), Moss (*Physcomitrella patens*; accession number XP001765592), and plants (*Arabidopsis thaliana*; accession number At4g26740, At2g33380, At1g70670, At1g23240, At1g70680, and At1g23250, *Cycas revoluta*; accession number FJ455154, and *Physcomitrella patens*; accession number XP001765592). These caleosin protein sequences were analyzed for phylogenetic

tree reconstruction using MEGA4 software with Neighbor joining system (bootstrap values from 100 replicates).

For physicochemical analysis, their physicochemical properties (*i.e.* theoretical isoeletricpoint (pI) and molecular mass) and topological model were analyzed from amino acid sequence using ProtParam and THMHMM softwares, respectively (http:// http://www.expasy.org/). In addition, several unique domains of caleosin (*e.g.* calcium-binding EF-hand and proline-knot motifs) were analyzed by interPro software (http://swissmodel.expasy.org/).

3.7.4 Expression of recombinant caleosin protein

3.7.4.1 Induction of recombinant caleosin protein

The expressing cells, *E. coli* strain BL21 carrying *caleosin*/pCold I plasmid were grown in LB medium supplemented with 50 µg/ml of ampicillin at 37°C until OD620 reached 0.4 to 0.6 (mid-logarithmic-phase) prior to keeping cells culture at low temperature (16 $^{\circ}$C) for 30 minutes. Expression of protein was induced by addition of 0.5 mM Isopropyl β-D-1-thiogalactopyranoside (IPTG) as per the manufacturer's instruction and further cultured at 16 $^{\circ}$C for 0, 3, 6, and 16 hours. After that, cells were harvested by centrifugation at 12,000 rpm for 5 min at 4 °C. The cell pellets were washed twice and resuspended in 100 mM Tris-Cl pH 8.0. Cells suspension was sonicated for cell breaking and then collected 50 µl of sonicated fraction as a cell lysate fraction. Remaining breaking cells were centrifuged again and transferred the clear supernatant to new microcentrifuge tubes as a supernatant fraction.

3.7.4.2 SDS-PAGE and Western Blot analysis

Both cell lysate and supernatant were used to analyze the expression level of *Chlorella* caleosin by SDS-PAGE (Appendix 3) and Western Blotting analysis (Appendix 4), respectively. Protein concentration was determined by Bradford method (Bradford, 1976) (Appendix 5). SDS-PAGE was performed by standard

protocol (Laemmli, 1970) using 12.5% or 15% polyacrylamide gel and stained with Coomassie brilliant blue R-250 (CBB). The molecular mass of recombinant caleosin protein was determined by comparing with protein molecular weight marker (Biorad, USA). Western Blotting analysis was carried out to confirm the recombinant caleosin protein was fused in-frame with six histidine tag at its N-terminus derived from pCold I vector. In this experiment, 30 µg protein of recombinant caleosin was separated by 12.5% SDS-PAGE and protein band was transferred to Polyvinylidene Fluoride (PVDF) membrane using blotting transfer buffer. Blotting was done after running (170 µg protein/cm^2) for one hour and followed by blocking in blocking solution for one hour with 100 ml of 1xPBS buffer plus 5% skim milk solution. Then, PVDF membrane was incubated with primary-antibody (an antibody raised against 6-histidine, 6X-His tag (R&D systems, USA)) for one hour and membrane was washed twice with 100 ml of 1x PBS buffer for 30 min by gently shaking. After washing, the membrane was incubated with secondary-antibody (an antibody raised against mouse conjugated with horseradish peroxidase (HRP) (Biolab, USA)) for one hour and washed twice with 100 ml of 1xPBS buffer for 30 min. The PVDF membrane was developed the signal by detection reagent for HRP (Biolab, USA) as per the manufacturer's instruction.

3.7.5 Purification of recombinant caleosin protein

In this study, caleosin was fused in-frame with six histidine tag at its N-terminus. Thereby, fusion protein could be purified by affinity chromatography using Hitrap FF column charged with Ni^{2+} (Ni-column 5 ml) (GE Healthcare Life Sciences, USA). As per manufacterer's instruction, 10 mg of total protein was mixed with binding buffer (total volume up to five milliliters). The mixture was filtrated through 0.45 µm filter, followed by loading into Ni-column. Purification was performed by AKTA prime system. Column was equilibrated and washed by binding buffer (10 mM imidazole and 1 M NaCl in 100 mM Tris-Cl pH 9). For the elution step, recombinant caleosin protein was eluted into fraction collector (1 ml/fraction) by using elution buffer (300 mM imidazole and 1 M NaCl in 100 mM Tris-Cl pH 8) using flow rate 1

ml/min, and 1 MPa pressure with linear gradient program. Eluted fractions were monitored the profile at absorbance 280 nm together with the analysis by SDS-PAGE. Then, target fractions containing recombinant proteins were pooled and desalted with 100 mM Tris-Cl pH 8 by Amicon Ultra-2 (Sigma, USA). Then, the purified fractions were again analyzed by SDS-PAGE.

3.7.6 Functional analysis of recombinant caleosin protein

3.7.6.1 Calcium binding (modified from Yuasa & Maeshima, 2000)

To test calcium binding property of recombinant caleosin protein, supernatant or purified fraction (obtained from 3.7.5) were incubated with 10 mM $CaCl_2$, 100 mM $CaCl_2$, 100 mM ethylene glycol tetraacetic acid (EGTA), and 100 mM $CaCl_2$ with 100 mM EGTA for 30 minutes at room temperature (Yuasa & Maeshima, 2000). Then, mobility shift on polyacrylamide gel was observed by Western Blotting analysis. Proteins were first separated on 15% SDS-PAGE and subjected to Western Blotting as described on 3.7.4.2.

3.7.6.2 Peroxygenase activity (modified from Hanano *et al*., 2006)

Both supernatant and purified fractions were used to measure peroxygenase activity. The reaction mixture contained 1 M phosphate buffer pH 7.2, 1 mM aniline as a substrate and 0.5 mg of total protein (supernatant or purified protein) (Hanano *et al.*, 2006). To start reaction, cumene hydroperoxide was added to yield final concentration of 0.1 mM. Product of peroxygenase activity was monitored by measuring the absorbance change at 310 nm within 30 min using spectrophotometer (Shimadzu, Japan). Peroxygenase activity was calculated and expressed as specific activity.

For dialysis experiment, 0.7 mg of supernatant protein was dialyzed against one liter of 100 mM Tris-HCl buffer pH 8 containing 1 mM EGTA for 16 hours.

Dialyzed protein was used in peroxygenase activity assay with measuring the absorbance change at 310 nm.

3.7.6.3 Hemoprotein (modified from Hanano *et al.*, 2006)

For hemoprotein characterization, heme spectrum was measured between 450-350 nm region (Soret band). The reaction contained 0.7 mg of supernatant protein and purified recombinant caleosin protein and 1 M phosphate buffer pH 7.2. Cumene hydroperoxide at final concentration 0.1 mM was added to inactivate of the protein (Hanano *et al.*, 2006).

3.7.7 Nile red staining (intracellular LD staining)

C. vulgaris TISTR 8580 cells were grown under control and stress conditions as described in 3.7.1.3. In each condition, one milliliter of cell culture at interval time (0-48 hr) was harvested by centrifugation at 12,000 rpm for 1 min. Cell pellets were re-suspended in 50 µl DMSO and stained with 2 µl of Nile red solution (100xdilution) (Appendix 6). Cell suspensions were immediately observed under fluorescent microscope for intracellular LD detection (Wagner *et al.*, 2010).

3.7.8 Semiquantitative RT-PCR for *Chlorella caleosin* gene

C. vulgaris TISTR 8580 cells were grown under condition as described in 3.7.1.3. Stressed cells were then harvested by centrifugation at 8,000 rpm for 10 min after 0, 24, and 48 hours, respectively. Total RNA was extracted using the RNeasy kit. Five µg of the total RNA was reverse transcribed into cDNA using the Superscript II RT (Invitrogen, CA, USA) as per the manufacturer's instruction. The PCR amplification was performed using primer sets: GGAGCCTGCGGCTTAATTTG, CvrRNA-F, and TCGCC AATCCGAACACTTCA, CvrRNA-R for *18S rRNA* gene as an internal positive control and ACCGCGACAACGACGGTGTGCTG, CvClo-F3, and TTAAAGACGTCAACCCGCCA,

CvClo_PCR-R for *Chlorella caleosin* amplification. The PCR products were analyzed by electrophoreses on 1.2 % (w/v) agarose gels with 0.1 μg/ml ethidium bromide staining. Statistical analysis was carried out using Gel Doc EZ Imager program (Biorad, USA).

3.8 Overexpression of *ACP* gene from *S. elongatus* PCC 7942

3.8.1 Strains and growth conditions

E. coli strain DH5α cells were grown in LB medium at 37°C as described in 3.7.1.1. *E. coli* transformed cells were grown under the same conditions as the wild-type cells but were supplemented with 50 μg/ml of ampicillin and streptomycin when they were transformed with pGEM-T Easy vector and shuttle vector pUC303, respectively. The growth of bacterial cells was monitored by measuring the absorbance at 620 nm.

Fresh water cyanobacterium, *S. elongatus* PCC 7942 cells were grown photoautotrophically (120 μE m^{-2} s^{-1}) in BG11 liquid medium (as normal condition) with shaking 150 rpm at 30°C. The growth of cyanobacterial cells was monitored by measuring the absorbance at 730 nm.

For salt stress condition, *S. elongatus* PCC 7942 cells were grown under the same conditions as culturing but 0.3 M of NaCl were added into BG11 liquid medium (hereafter salt-stress medium).

3.8.2 Construction of *ACP* from *S. elongatus* PCC 7942

Genomic DNA was extracted from 100 mg fresh weight of *S. elongatus* PCC 7942 cells using the DNeasy Plant mini kit as per the manufacturer's instruction. The genomic DNA quality was checked by electrophoresis on 1.0 % (w/v) agarose gel with 1: 10,000 dilution of SYBR safe DNA gel stain. Extracted DNA was monitored by

measuring the absorbance at 260/280 nm with NanoDrop 2000 UV-Vis Spectrophotometer. Putative *ACP* together with its native promoter was amplified by PCR from genomic DNA of *S. elongatus* PCC 7942 using specific primer pair: GTGACTGGAACCGCCCTCGCG, ACP_7942_F, and TTAACTCGCCGATTCAAACAT, ACP_7942_R which introduced *Bam*HI and *Xho*I restriction sites on the 5' and 3' ends. PCR product size approximately 2.3 kb was clone into pGEM-T Easy vector. DNA fragments of *ACP* with its native promoter were prepared by double digestion with *Bam*HI and *Xho*I and ligated into the corresponding sites of pUC303 vector (Kuhlemeier & van Arkel, 1987) (Figure 8). The recombinant plasmid, 2.3 kb of *ACP7942* fragment was further ligated into pUC303 vector (hereafter *ACP7942*/pUC303). Recombinant plasmid *ACP7942*/pUC303 was used to transform into *E. coli* DH5α cells as standard protocol (Sambrook *et al.*, 1989). To check candidate clones, colony PCR was performed using specific primers for *ACP* and streptomycin gene primers amplification. Positive clones for *ACP* and streptomycin were extracted from *E. coli* cells using PureLink Quick Plasmid Miniprep kit. Restriction enzyme analysis by using *Bam*HI and *Xho*I was performed as per manufacterer's instruction for second confirmation.

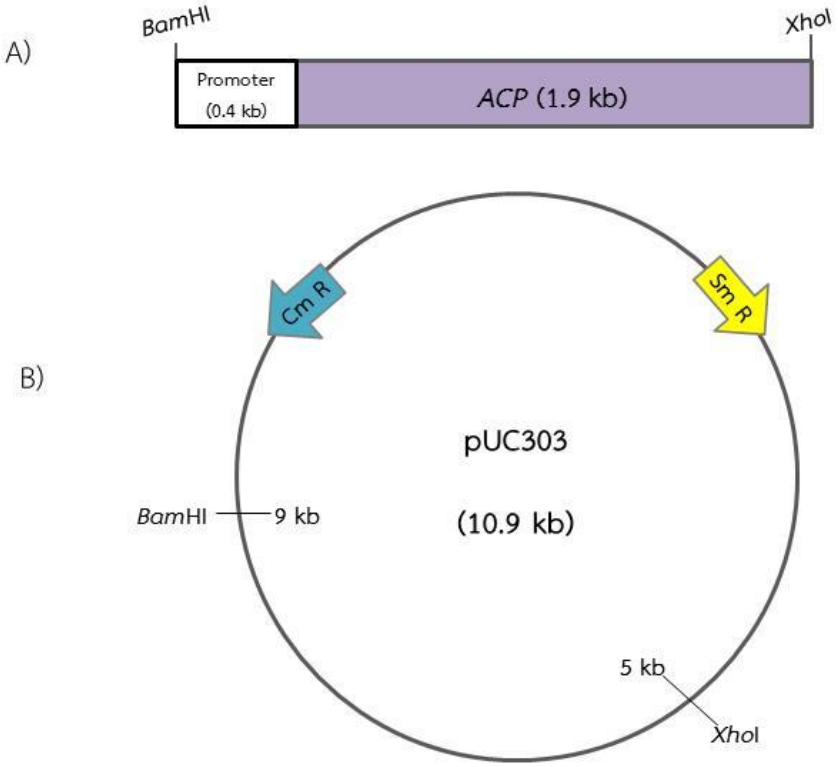

Figure 8: Schematic for *ACP* construction. A) Contruction of ACP from *S. elongatus* PCC 7942 and its native promoter B) Vector pUC303 (modified From; Kuhlemeier and Arkel, 1987) used as a shuttle vector for expression.

3.8.4 Transformation into *E. coli*

One hundred microliters of *E. coli* DH5α competent cells were thawed on ice. After that, purified recombinant plasmids, *ACP7942*/pUC303, approximately 100 ng were added into competent cells. The transformation mixture was flicked 2-3 times and was stood on ice for 10 min. Then, the mixture was heated to 42 °C for 90 second and stood on ice for 5 min. Then the mixture was diluted with 900 µl of LB medium and gently shaking at 37 °C for 60 min. Cell suspension was spreaded and selected on LB agar containing streptomycin at final concentration 50 µg/ml. The single colony was re-streaked on new selective LB agar for inserted plasmid confirmation then positive clones were transferred to liquid LB medium for large scale culturing.

3.8.5 Transformation into *S. elongatus* PCC 7942

Recombinant plasmid *ACP7942*/pUC303 was transformed into wild-type strain *S. elongatus* PCC 7942 as previously describe (Nomura *et al.*, 1995). Briefly, 5 ml of *S. elongatus* PCC 7942 (Absorbance at 730 nm approx. 0.5) culture cells were harvested by centrifugation at 4,500 rpm for 10 min. Cells pellet were then washed by fresh BG11 medium for at least three times. The washed cells were re-suspended in one milliliter of BG11 medium. One hundred microliters of cells suspension were mixed with 300 ng plasmids, *ACP7942*/pUC303 as overexpressing cells and pUC303 as control cells. The mixtures were incubated at 30°C in dim light for overnight. BG11 medium was added into the mixture up to 300 µl. Then, the cell mixtures were laid onto BG11 plates. Transformed cells were grown under the same conditions as the wild-type cells for five days. Candidate transformants were selected by addition of 50 µg/ml streptomycin. After 21 days, several single colonies were re-streaked on BG11 supplemented with streptomycin. To candidate transformants, cells of candidate clones were used as a template DNA in colony PCR analysis by using specific primers for *ACP* and streptomycin amplification. The PCR products band intensity was carried out using Gel Doc EZ Imager program (Biorad, USA).

3.8.6 Lipid profile analysis

Transformant *S. elongatus* PCC 7942 cells were grown under normal- and stress-conditions as described in 3.8.1. Four hundred milliliters of transformant liquid cultures were grown for 14 days with 50 µg/ml of streptomycin supplementation under above conditions. After that, cells were harvested by centrifuged at 8,000 rpm for 10 min. Harvested cells were washed at least three times by new liquid media. Then, washed cells were dehydrated by freezed drying (Flexi-Dry MP, Kinetics, USA) before lipid analysis.

For esterification of extracted fatty acid, two milliliters of methanol-hydrochloric 95:5 (v/v) was added to approximately 50 mg cells dried weight then

mixed and incubated at 80 - 85 ^{o}C for 90 min. One milliliter of distilled water was added to the mixture. For fatty acid methyl esters (FAME) extraction, FAMEs were extracted by hexane containing 0.01 % butylated hydroxytoluene (BHT) at room temperature. Reaction products were centrifuged at 4,000 rpm for 5 min to separate the organic and aqueous phases. Then, aqueous phase was selected and mixed with Na_2SO_4 for remaining water absorption. FAMEs were evaporated to dryness at room temperature under a gentle stream of nitrogen. The residue was solubilized again in 1 ml of hexane and analyzed it by gas chromatography.

FA were chromatographed as methyl esters on a 3 meter of HP-INNOWax column with an internal diameter of 0.25 μm. Agilent 6890N gas chromatograph (Agilent technologies, USA) equipped with a flame ionization detector (FID). Analysis was performed as following condition, helium carrier gas was performed as a mobile phase. The injector and detector temperature were maintained at 250 ℃. The oven temperature was started at 150 ℃ and then increased to 250 ℃ with increasing rate 10 ℃ per min. For analysis, fatty acids were compared with fatty acids standard.

CHAPTER IV
RESULTS

4.1 Expression and functional analysis of *caleosin* gene from *C. vulgaris* TISTR 8580

4.1.1 Bioinformatics analysis

The full length of *caleosin* (approximately 837 bp) was successfully isolated from *C. vulgaris* TISTR 8580 by RACE-method. Amino acid sequence of *Chlorella* caleosin in this study was shown in Figure 9. The deduced polypeptide comprises of 279 amino acid residues. In addition, several putative domains were found by protein domain analysis via EXPAXY server as described in 3.7.1. *Chlorella* caleosin protein consists of a single site for calcium-binding EF-hand motif at amino acid positions 73 to 99. Proline-knot motif is predicted at amino acid positions 24, 28, 30, and 33. Two putative histidines are found at amino acid positions 76 and 144 (Figure 9). Moreover, signature caleosin protein matching is found from amino acid positions 68 to 240 (data not shown). There is the unique amino acid insertion as shown in Figure 9 A.

Physicochemical property of *Chlorella* caleosin protein was analyzed from its amino acid sequence using ProtParam software (Artimo *et al.*, 2012). Theoretical isoeletricpoint (pI) and molecular mass of *Chlorella* caleosin protein are 8.54 and 31,047.2 Da (31.05 kDa), respectively. In addition, topology of *Chlorella* caleosin protein was predicted via TMHMM software as shown in Figure 4.2. According to protein hydrophobicity, there are three protein regions including inside membrane, outside membrane, and only one transmembrane segment. *Chlorella* caleosin protein appears only one transmembrane segment at the center position.

1 MVSASQMMANAPAGQSKKGQALVTTVDSVPVTKQHATIDVSDRLHNPGMPRANVTCDAEH 60

61 PHGTYSPPNMTVMQQHIAFWDRDNDGVLWPQDTYVGFRKLGFNVLLSAIAVPVIHGTFSW 120

121 WTGPSWIPDPAMRIYMKNIHRGKHGSDSETYDTEGRFVPQKFEEIFSKYDHGGKGGLTLS 180

181 EVNEMIRGNRNIMDPVGWVAGWLEWNTSFYLIAKDTPRGRLLLKDDMRAIIDGTIFYRLA 240

241 REVEEGRLKQKQVHGGMKKAKGPDAGRGLTAQAAGAKEE 279

Figure 9: Amino acid sequence of *Chlorella* caleosin protein. Full length of *caleosin* was isolated from *C. vulgaris* TISTR 8580 by RACE-method. The deduced polypeptide comprises of 279 amino acid residues. Several protein domains were analyzed using interPro software. Underline denotes the putative calcium binding motif. The blue highlight of Histidine76 and Histidine144 represent the putative histidines which were involved in the histidine-dependent peroxygenase activity. Stars denote the putative proline-knot motif and amino acids boxed indicated the unique insertion.

Other amino acid sequences from fungi, green algae, moss, and plant caleosin proteins were obtained from databases. Physicochemical properties (*i.e.* pI and molecular mass) of caleosin proteins were compared and shown in Table 1. These 16 caleosin protein sequences clustered into three main groups when phylogenetics analysis was performed (Neighbor-joining tree) using MEGA4 software (Figure 11).

First group consisted of *A. thaliana* (At4g26740), (At2g33380), (At1g70670), (At1g70680), (At1g23250), and *C. revoluta* (FJ455154). In this group, all members are plant origins. Second group consisted of *N. crassa* (Q7S2T2), *C. vulgaris* TISTR 8580, and *A. thaliana* (At1g23240) and third group consisted of *M. oryzae 70-15* (XP_365887)*, U. maydis* (Q4PAW0), *A. protothecoides* (AEB77763), *C.subellipsoidea* C-169 (EIE19761.1), (EIE19762.1), *V. carteri* (XP_002958325.1), and *P. patens* (XP001765592). For second and third groups, their members are fungi, green algae, moss, and plant origins.

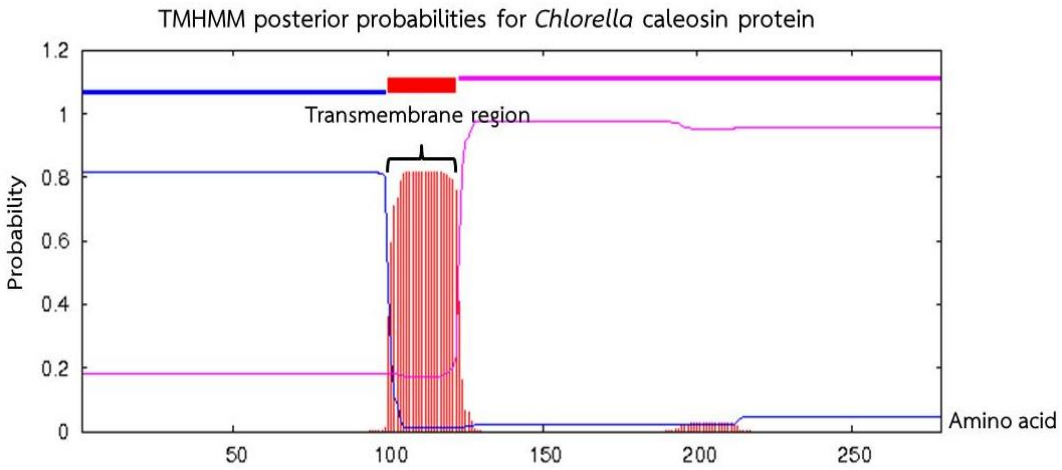

Figure 10: Topological model of *Chlorella* caleosin protein was predicted using TMHMM software (ExPASy server). Blue line denotes the inside membrane region, pink line denotes the outside membrane region, and red line denotes the transmembrane protein region.

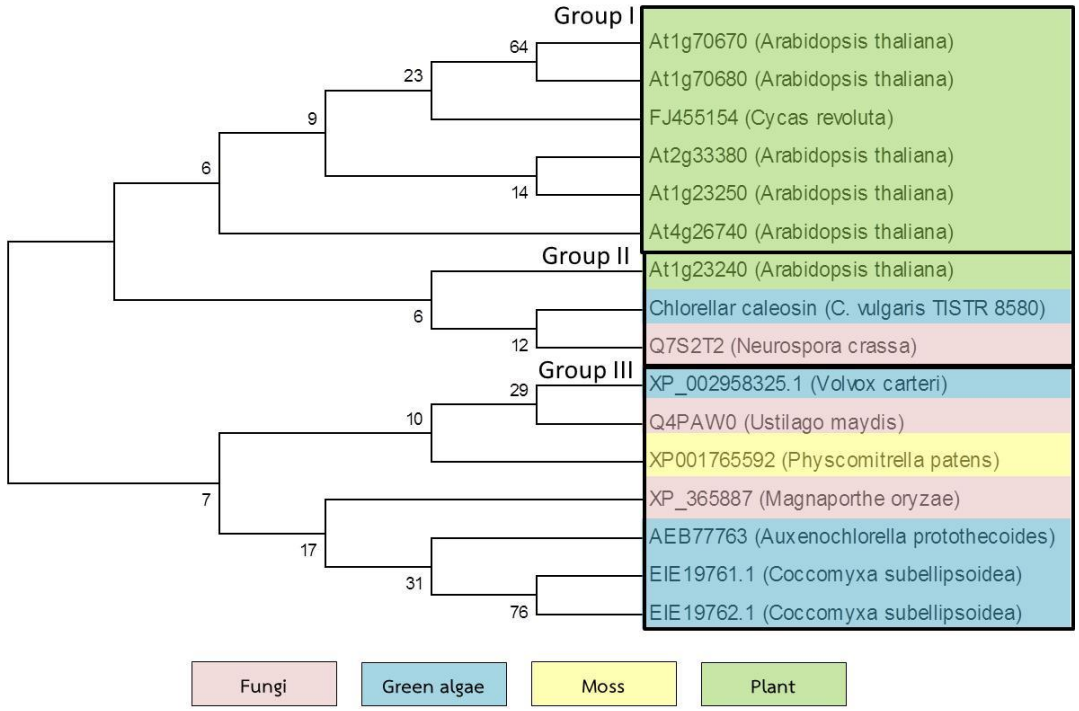

Figure 11: Phylogenetic analysis of caleosin protein sequences. A phylogenetic tree was constructed using an alignment of full-length protein sequences generated using MEGA4 software with bootstrap values from 100 replicates. Pink boxes represent fungi group, blue boxes represent green algae group, yellow box represents moss group, and green boxes represent plant group.

Table 2**:** Physicochemical properties of caleosin proteins.

Group	Organisms (Accession number)	Amino acid residue	pI	Molecular mass (kDa)
Fungi	*Magnaporthe oryzae 70-15* (XP_365887)	247	5.7	28.3
	Neurospora crassa (Q7S2T2)	299	5.2	34.2
	Ustilago maydis (Q4PAW0)	252	7.1	28.8
Green algae	*Auxenochlorella protothecoides* (AEB77763)	252	6.5	29.1
	C. vulgaris TISTR 8580	279	8.5	31.0
	Coccomyxa subellipsoidea C-169 (EIE19761.1)	248	6.5	27.5
	Coccomyxa subellipsoidea C-169 (EIE19762.1)	254	9.0	29.1
	Volvox carteri (XP_002958325.1)	241	6.7	27.8
Plants	*Arabidopsis thaliana* (At4g26740)	245	5.8	28.0
	Arabidopsis thaliana (At2g33380)	236	5.2	26.6
	Arabidopsis thaliana (At1g70670)	195	9.4	22.1
	Arabidopsis thaliana (At1g23240)	210	9.6	23.9
	Arabidopsis thaliana (At1g70680)	192	9.0	21.5
	Arabidopsis thaliana (At1g23250)	205	9.8	23.8
	Cycas revoluta (FJ455154)	235	6.7	26.8
Moss	*Physcomitrella patens* (XP001765592)	248	6.3	28.4

4.1.2 Expression of recombinant caleosin protein

In this study, *caleosin* gene was expressed under cspA promoter (pCold system). *E. coli* expressing cells (strain BL21 harboring *caleosin*/pCold I) were grown and induced protein expression by IPTG. After IPTG induction, cells were harvested and sonicated. Both supernatant and cell lysate fractions were analyzed by SDS-

PAGE using 12.5% polyacrylamide gel and stained with CBB. As shown in Figure 12 A, significant amount of 32 kDa protein was detected after IPTG induction for 3, 6, and 16 hours. The observed molecular mass is in good agreement with the theoretical molecular mass of the *Chlorella* caleosin. The recombinant protein was found in both supernatant and cell lysate fractions. To confirm the recombinant caleosin protein fused-in-frame with 6X-His tag, supernatant fraction was analyzed by Western Blotting using antibody raised against 6X-His tag as described in Materials and Methods. As shown in Figure 12 B, the 32 kDa protein exhibited a single cross-reaction band. The *E. coli* cells transformed with the vector alone did not show any cross-reaction band (data not shown). These results indicated the *Chlorella* caleosin was able to expressed in *E. coli*.

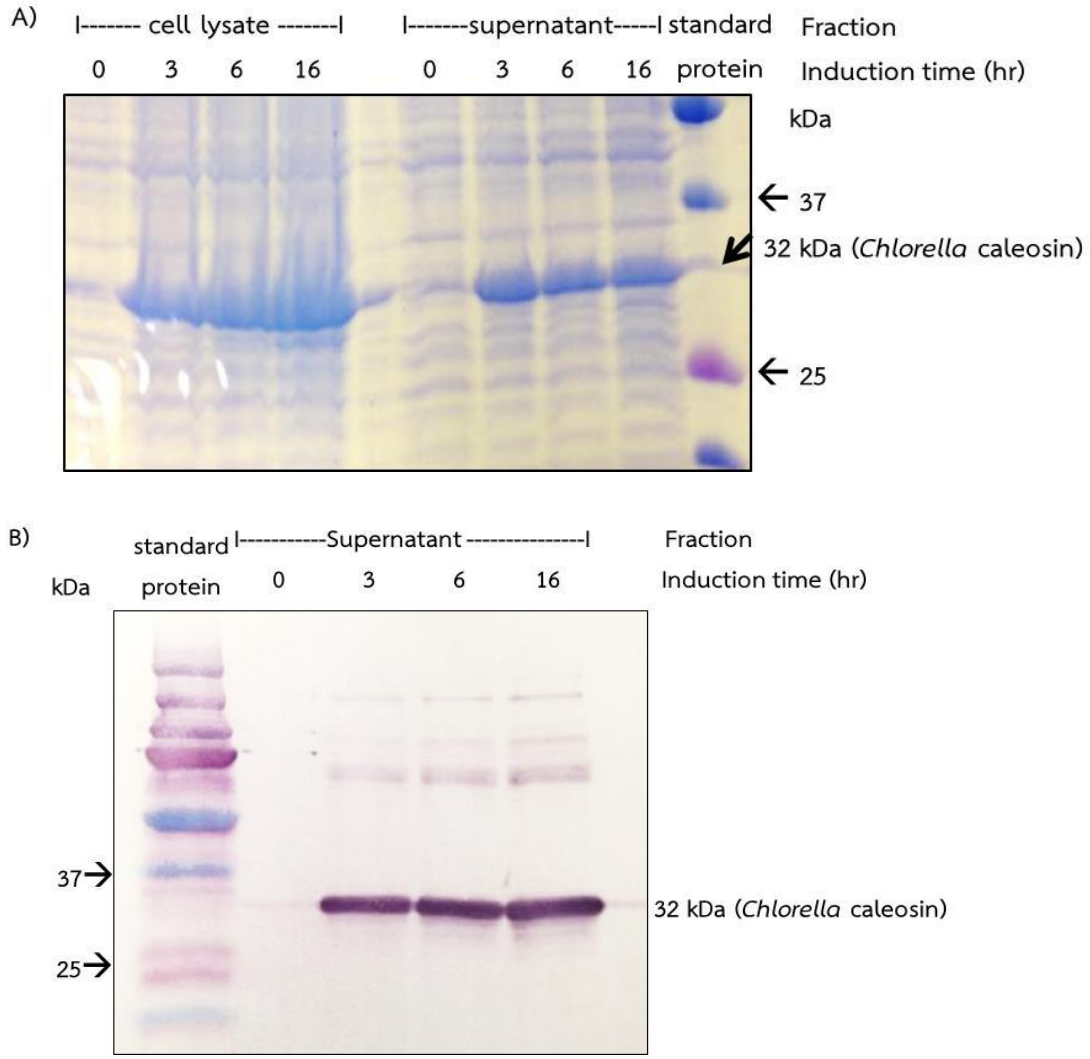

Figure 12: Expression of recombinant caleosin protein from *C. vulgaris* TISTR 8580 in *E. coli* BL21. Harvested cells were broken by sonication, cell lysate fractions were collected, and remaining cell lysate was centrifuged to obtain supernatant fractions. Equal amount of proteins (50 µg) were applied per lane. (A) SDS-PAGE analysis of cell lysate and supernatant fractions after IPTG induction (0, 3, 6, and 16 hr) which was performed on 12.5 % acrylamide gel and stained with CBB, (B) Western blotting of supernatant fractions after IPTG induction was performed on PVDF membrane. Mouse antibody raised against 6X-His tag and antibody raised against mouse conjugated with HRP were used as primary and secondary antibodies, respectively.

4.1.3 Purification of recombinant caleosin protein

Recombinant caleosin protein was purified using 5 ml size of Hitrap FF column charged with Ni^{2+} (Ni-column) as per manufacterer's instruction. Briefly, recombinant protein was resuspended in 100 mM Tris-Cl pH8, filtrated, and applied into the equilibrated column with binding buffer containing 10 mM imidazole and 1 M NaCl in 100 mM Tris-Cl pH 9. Non-binding proteins were washed by binding buffer. Finally, binding recombinant caleosin proteins were eluted into fraction collector (1 ml/ fraction) by elution buffer containing 300 mM imidazole 1 M NaCl in 100 mM Tris-Cl pH 8 using 1 ml/min of flow rate, and 1 MPa pressure with linear gradient program. Profile of protein elution was shown in Figure 13. Purified protein peak appeared around fractions 17 to 20 when Elution buffer gradient was 100% thus recombinant caleosin proteins could be eluted with 300 mM imidazole, these eluted fractions were further checked by SDS-PAGE (Figure 14 A). The results show only 32 kDa protein bands. Then, purified protein fractions were pooled and desalted with 100 mM Tris-Cl pH8. Purified protein was again analyzed by SDS-PAGE comparing with non-purified supernatants which obtained from control cells, harbouring pCold I empty vector and expressing cells, harbouring *caleosin*/pCold I. As shown in Figure 14 B, purified recombinant caleosin protein had only one band at 32 kDa.

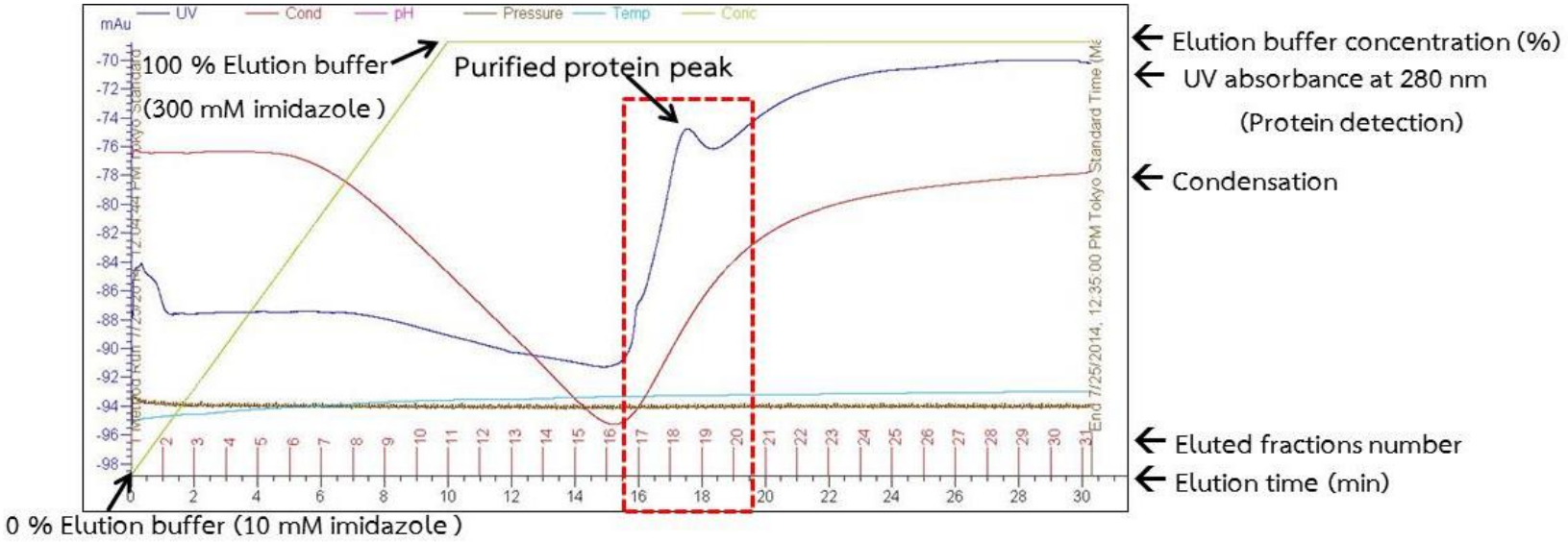

Figure 13: Protein elution profile from recombinant *chlorella* caleosin purification by AKTA prime. These profiles shown linear gradient of elution buffer (0-100%) as green line, and blue line represented as UV absorbance of protein (280 nm). Purified protein peak appeared around fractions 17 to 20. Green line: elution buffer concentration; blue line: UV absorbance at 280 nm; red line: column condensation.

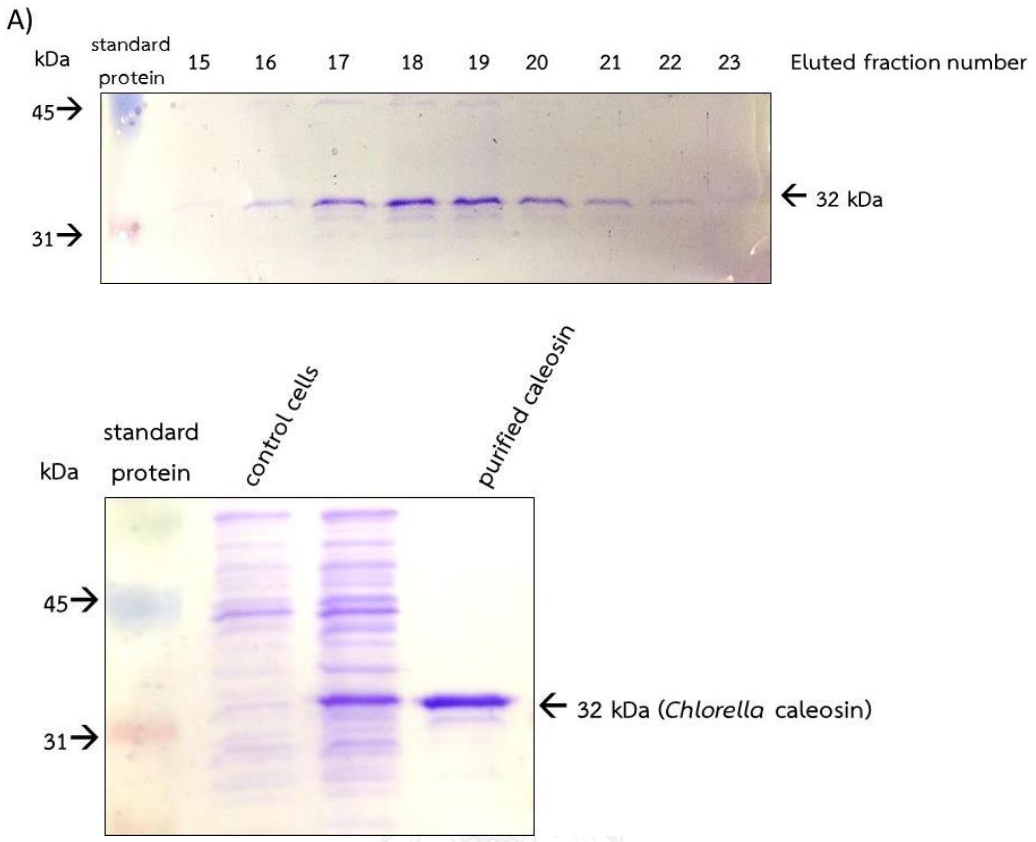

Figure 14: Purification of recombinant *Chlorella* caleosin protein by Ni-column. Ten milligrams of total protein in supernatant which resuspended in 100 mM Tris-Cl pH8 was filtrated, and loaded into column (5 ml column size). Binding buffer contained 10 mM imidazole and 1 M NaCl in 100 mM Tris-Cl pH 9 was used to equilibrate and wash the purified system. Elution buffer contained 300 mM imidazole 1 M NaCl in 100 mM Tris-Cl pH 8 was used to elute binding recombinant caleosin proteins into the fraction collector tubes by linear gradient. The eluted fractions were selected from protein elution profile and checked by SDS-PAGE analysis. (A) SDS-PAGE analysis of eluted fractions. Ten microliters from each eluted fraction (fractions 15 – 23) were directly separated on 12.5 % acrylamide gel and protein bands were stained with CBB, and (B) SDS-PAGE analysis of purified caleosin protein, compared with non-purified supernatants. Equal amount of proteins (10 µg) of supernatant from E. coli cells carrying empty vector, supernatant from E. coli cells carrying caleosin/pCold, and purified recombinant caleosin protein were applied per lane. Protein bands were separated on 12.5 % acrylamide gel and stained with CBB for protein detection, respectively.

4.1.4 Functional analysis of recombinant caleosin protein

4.1.4.1 Calcium binding

Purified recombinant caleosin protein obtained from 4.1.3 was further used for functional analysis.

Firstly, for calcium bind activity, 10 μg of total protein in supernatant and purified proteins were treated with $CaCl_2$ and/or EGTA as described in 3.7.5.1. Then, the reactions were analyzed by Western Blotting to detect mobility shift. The result of purified caleosin protein experiment shown in Figure 15, all treatments had same protein mobility when compared with native purified caleosin protein that shown no mobility shift by calcium binding activity. Supernatant was also tested and the result was similar to purified caleosin protein (data not shown).

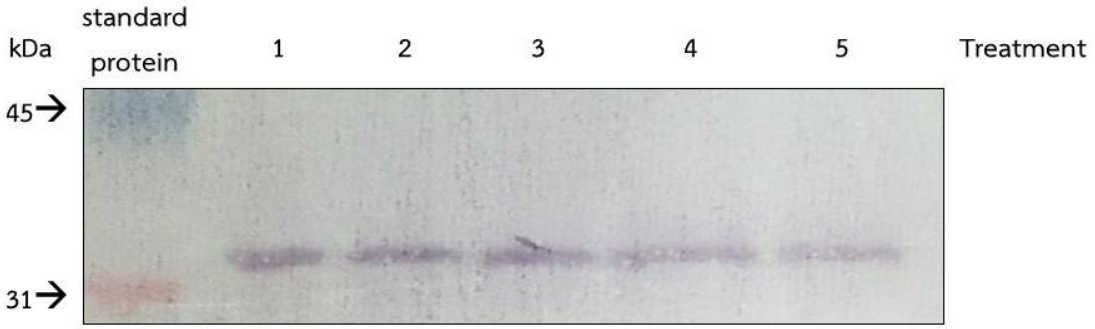

Figure 15: Western Blotting analysis of mobility shift with calcium binding activity. Western Blotting was performed to investigate the mobility shift of purified protein with calcium binding activity. Purified protein (10 µg) was treated by incubation for 30 minutes at room temperature with 10 mM $CaCl_2$, 100 mM $CaCl_2$, 100 mM EGTA, and 100 mM $CaCl_2$ with 100 mM EGTA, respectively. Proteins were separated on 15% polyacrylamide gel and transferred into PVDF membrane. For immunoloblotting, Antibody raised against 6X-His tag and antibody raised against mouse conjugated with HRP were used as primary and secondary antibodies, respectively. Then, cross-reaction band was visualized by HRP detecting reagent and the mobility shift was carried out by protein mobility comparison.

lane 1: purified recombinant caleosin protein (10 µg) in the absence of $CaCl_2$ and EGTA,

lane 2: purified recombinant caleosin protein (10 µg) in the presence of 10 mM $CaCl_2$,

lane 3: purified recombinant caleosin protein (10 µg) in the presence of 100 mM $CaCl_2$,

lane 4: purified recombinant caleosin protein (10 µg) in the presence of 100 mM $CaCl_2$ with 100 mM EGTA, and

lane 5: purified recombinant caleosin protein (10 µg) in the presence of 100 mM EGTA.

4.1.4.2 Peroxygenase activity

Secondly, function of peroxygenase was examined in recombinant caleosin protein. Peroxygenase activity was assayed using both supernatant and purified protein from 4.1.3. Aniline was used as a substrate for hydroxylation reaction. The reaction mixture contained 1 M phosphate buffer pH 7.2, 1 mM aniline as a substrate and 0.5 mg of total protein in the presence of supernatant or purified recombinant caleosin protein. To start reaction, cumene hydroperoxide was added to yield final concentration 0.1 mM, then product of peroxygenase activity, nitrosobenzene was monitored by measuring the absorbance change at 310 nm within 30 min. For time course experiment, reaction mixture was monitored at absorbance 310 nm. Initially, the absorbance was stable; however, the absorbance increased gradually after cumene hydroperoxide was added (data not shown) because the reaction was started. Supernatant from control cells harbouring empty vector was analyzed as a negative control. Their specific activity values were compared, showing in Figure 16 A. Specific activity values of recombinant caleosin proteins (supernatant and purified recombinant caleosin protein) were 0.09 ± 0.01 unit/min/mg protein and 0.06 ± 0.01 unit/min/mg protein, respectively. These specific activity values were higher than control ones (0.00 ± 0.00 unit/min/mg protein) approximately 216 and 134 folds, respectively. Interestingly, specific activity of purified protein was decreased approximately 1.6 folds when compared with supernatant protein. For dialysis experiment, supernatant was dialyzed by incubation for 16 hour with one liter of 100 mM Tris-HCl buffer pH 8 containing 1 mM EGTA. Then, dialyzed supernatant protein was measured the peroxygenase activity as shown in Figure 16 B. After dialysis, specific activity decreased from 0.09 ± 0.01 unit/min/mg protein to 0.06 ± 0.01 unit/min/mg protein. It was decreased approximately 1.6 fold when compared with before dialysis. Next, dialyzed protein

was mixed with 10 mM $CaCl_2$ and the mixture was examined for peroxygenase assay. As the result, specific activity of dialyzed protein could not be recovered by 10 mM $CaCl_2$ addition (0.05 ± 0.00 unit/min/mg protein).

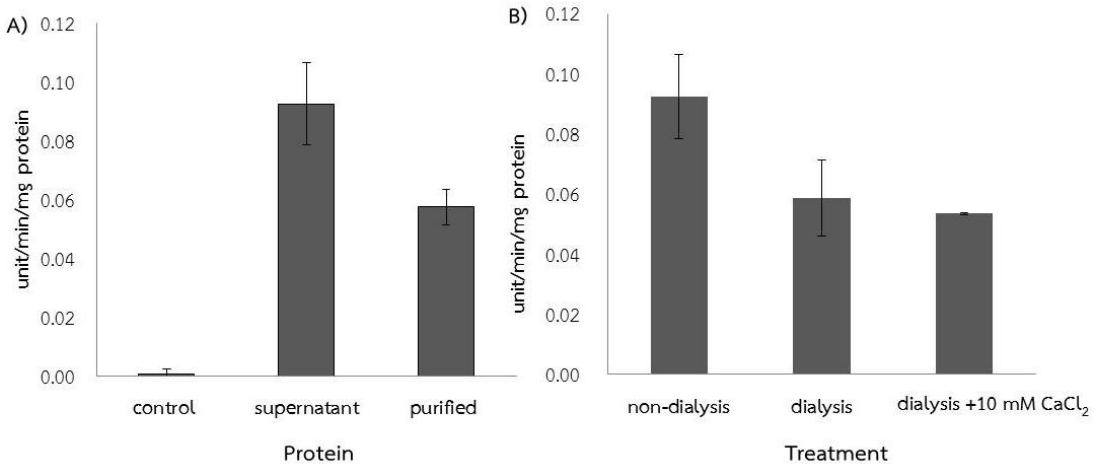

Figure 16: Comparison of peroxygenase activity. For peroxygenase experiment, 0.5 mg of supernatant (from *E.coli* harbouring empty vector (pCold I) and *caleosin*/pCold I) or purified recombinant caleosin proteins were used in the reaction containing 1 M phosphate buffer pH 7.2, 1 mM aniline as a substrate, and 0.1 mM cumene hydroperoxide as reaction starter. Then, oxidation product of peroxygenase activity, nitrosobenzene was monitored by measuring the absorbance change at 310 nm within 30 minutes. For dialysis, proteins were dialyzed against one liter of 100 mM Tris-HCl buffer pH 8 containing 1 mM EGTA for 16 hour and these dialyzed proteins were used to test in peroxygenase experiment, (A) specific activity before dialysis, and (B) specific activity after dialysis and in the presence of 10 mM $CaCl_2$. Data are means ± standard deviation of three independent experiments.

4.1.4.3 Hemoprotein

Thirdly, hemoprotein property also was examined using recombinant caleosin protein. Seven hundred micrograms of supernatant and purified recombinant caleosin proteins were applied into hemoprotein assay reaction containing 1 M phosphate buffer pH 7.2. Then, Heme spectrum was measured the absorbance between 450-350 nm (Soret region) by spectrophotometer. Recombinant caleosin protein observed a heme peak or Soret band at the 407 nm region as shown in Figure 17 (upper line). To inactive heme region, the starter of peroxygenase activity, cumene hydroperoxide (final concentration 0.1 mM) was added in the

normal reaction and the spectrum was measured again. Addition of cumene hydroperoxide resulted in the decrease of this peak in both supernatant and purified proteins (Figure 17: lower line).

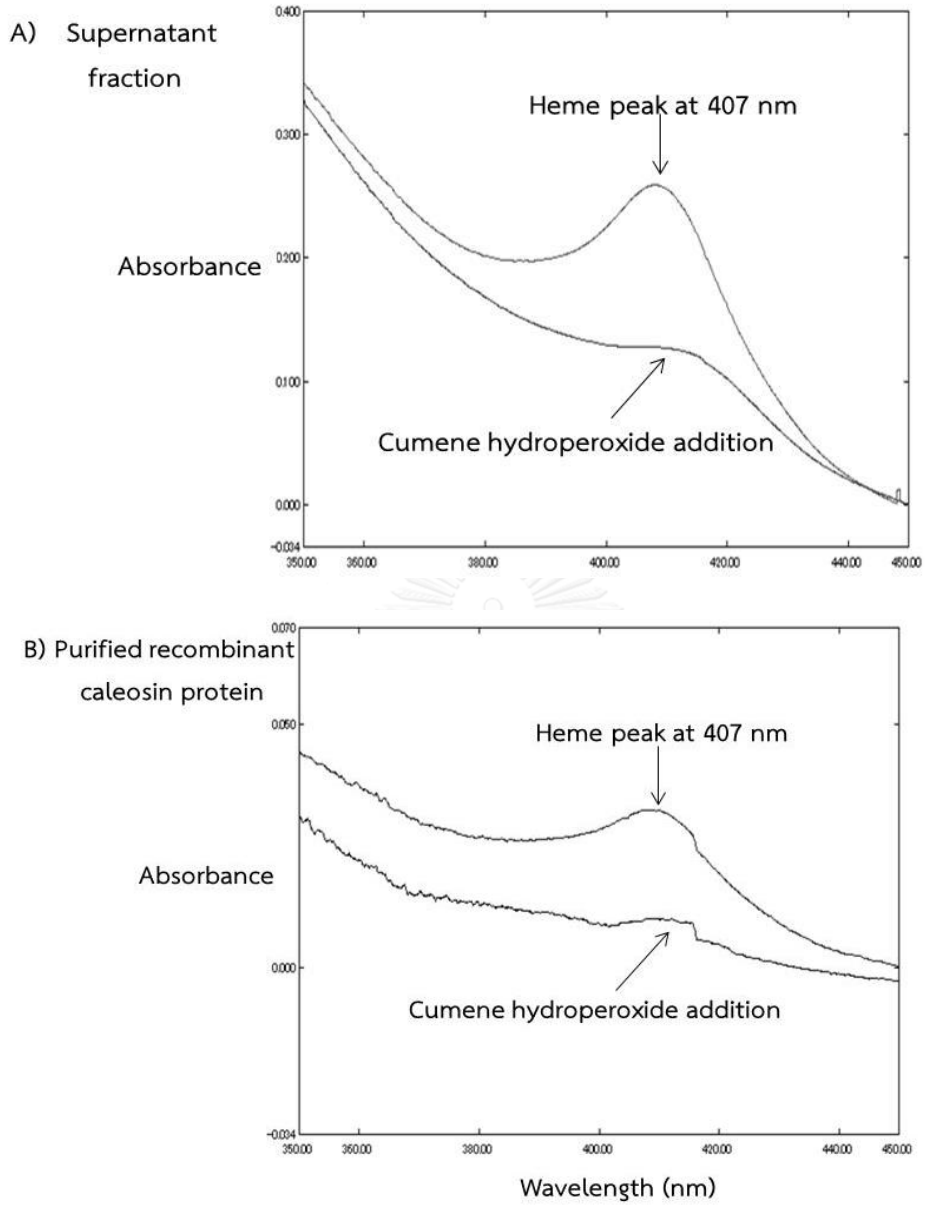

Figure 17: Spectrum of hemoprotein and inactivation of hemoprotein by cumene hydroperoxide addition. Hemoprotein assay reaction contained 0.7 mg of supernatant and purified recombinant caleosin proteins and 1 M phosphate buffer pH 7.2 (active heme region). The mixture reaction was measured the absorbance between 450-350 nm to observe Soret region by spectrophotometer. For inactivation of heme region, 0.1 mM cumene hydroperoxide were added in the normal reaction. Spectrum of active and inactive heme region were compared each other. (A) spectrum of supernatant fraction, and (B spectrum of purified recombinant caleosin protein.

4.1.5 Nile red staining in *C. vulgaris* TISTR 8580

To investigate intracellular LDs in *C. vulgaris* TISTR 8580, cells were grown under nitrogen deficiency, salt stress, and sodium acetate stress conditions for 0, 24, and 48 hours, respectively. Control and stressed cells were harvested, stained with Nile red solution as described in 3.7.6., and immediately observed under fluorescent microscope. Microscopic results shown in Figure 18, intracellular LDs were stained with Nile red as yellow. In normal growth condition, LDs were not detected in *C. vulgaris* TISTR 8580 (Figure 18 A-C). On the other hand, under stress conditions LDs could be observed clearly. For nitrogen deficient conditions (Figure 18 D-F) and salt-stress conditions (Figure 18 G-I), some amount of LDs could be detected after 24 hours and large amount of LDs appeared after 48 hours. It has been shown that at 48 hours of stresses, LDs accumulation in salt-stress condition was slightly higher than nitrogen deficiency. Larger amount of LDs were detected in sodium acetate stress condition significantly after 48 hours. It should be noted that *Chlorella* cell size was bigger than other conditions (Figure 18 J-L).

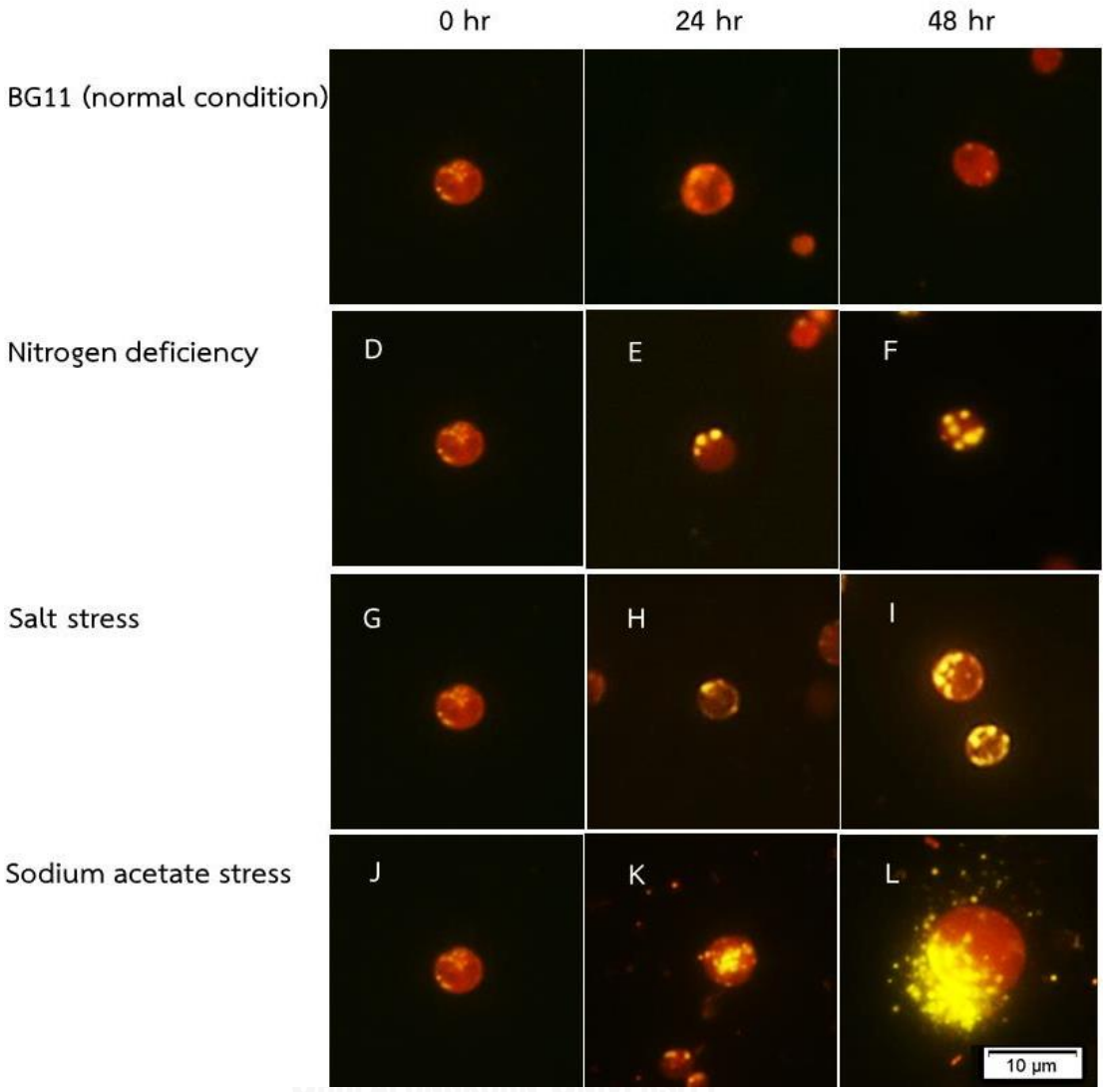

Figure 18: Nile red staining of *C. vulgaris* TISTR 8580 cells after growth in various stress conditions for 0, 24, and 48 hours. C. vulgaris TISTR 8580 cells were grown under normal condition until A730 reached 0.4. Then cells were transferred to nitrogen deficiency, salt stress, and sodium acetate stress conditions. Nile red staining was performed and observed immediately under fluorescent microscope for intracellular LD detection. (A-C) normal condition, (D-F) nitrogen deficiency, (G-I) salt stress, and (J-L) sodium acetate stress.

4.1.6 Semiquantitative RT-PCR of *caleosin* gene in *C. vulgaris* TISTR 8580

According to the technical problem of sodium acetate stress condition, *Chlorella* cells were slime sediments after cells harvesting. Thereby, only nitrogen deficiency and salt stress conditions were further studied by semiquantitative RT-PCR. *C. vulgaris* TISTR 8580 cells were grown under nitrogen deficiency and salt stress conditions for 0, 6, and 12 hours, respectively. Cells were collected by centrifugation. Total RNAs were extracted and reverse transcribed into cDNA as described in 3.7.7. For PCR amplification, *18S rRNA* gene was used as an internal control. The PCR products were analyzed by electrophoresis. Band intensity was measured by Gel Doc EZ Imager program (Bio-Rad, USA). Gel electrophoresis results shown as Figure 19 A, internal control gene had similar bands intensity in all conditions tested. For *Chlorella caleosin* gene, the intensity of PCR products were stronger than initial time (0 hour) after culturing under nitrogen deficiency and salt stress conditions for 6 and 12 hours, respectively. For statistical analysis, the results were shown in Figure 19 B and C. internal control had same relative value in all conditions which was consistent with electrophoresis results (Figure 19 B). Corresponding with electrophoresis results, relative values of *Chlorella caleosin* gene expression level were increased after 6 and 12 hours culturing under nitrogen deficiency and salt stress conditions. As shown in Figure 19 C, *Chlorella caleosin* gene was up-regulated under both stress conditions. For instance, the relative values of nitrogen deficiency and salt stress conditions at 12 hours were 4.24 ± 1.56 % and 6.46 ± 0.60 %, respectively. Thus, it was up-regulated approximately 3.8 and 6.5 folds under nitrogen deficiency and salt stress conditions, respectively.

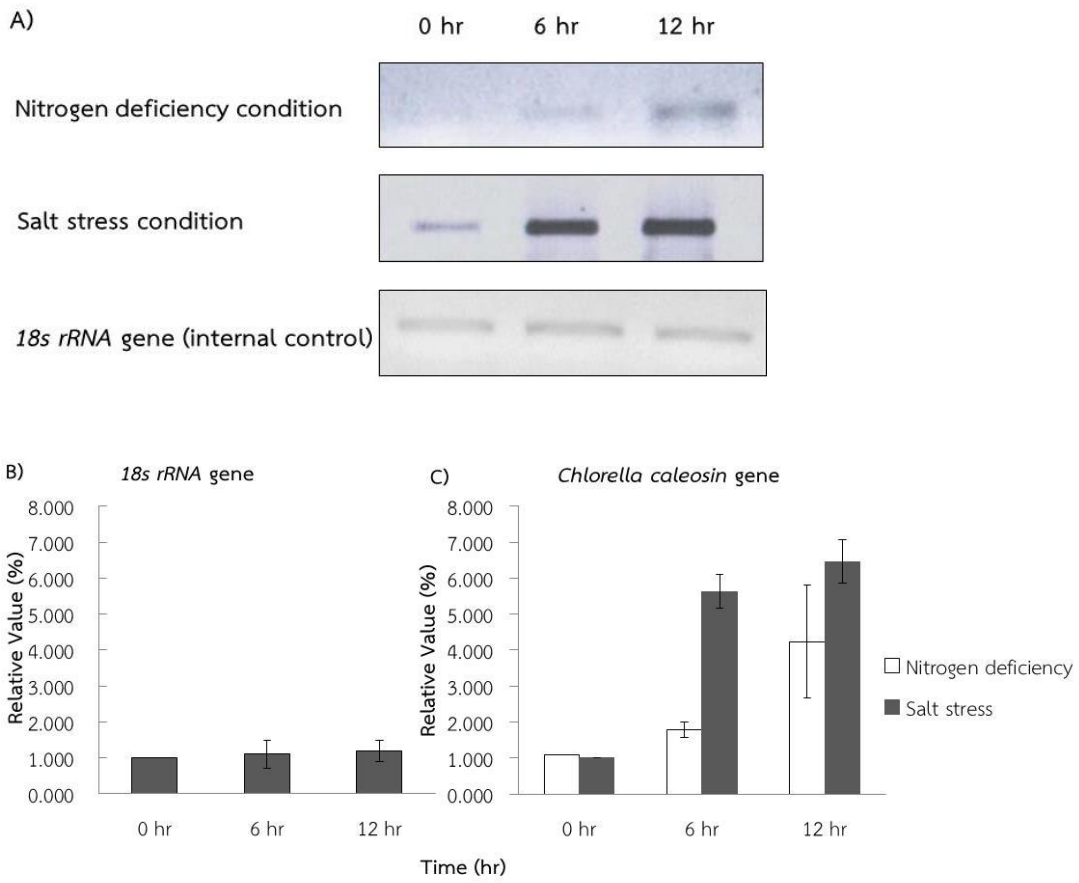

Figure 19: Semiquantitative RT-PCR of *Chlorella caleosin* gene under nitrogen deficiency and salt stress conditions. *C. vulgaris* TISTR 8580 cells after culturing under nitrogen deficiency and salt stress conditions for 0, 6, and 12 hours were harvesting. Total RNA was extracted and reverse transcribed into cDNA to use in PCR amplification of *18S rRNA* gene (internal positive control) and *Chlorella caleosin* gene. The PCR products were analyze by electrophoresis using 1.2 % (w/v) agarose gels with 0.1 µg/ml ethidium bromide staining. The band intensity was analyzed by Gel Doc EZ Imager program. (A) electrophoresis result, (B) band intensity analysis of *18S rRNA* gene (control), and (C) band intensity analysis of *Chlorella caleosin* gene (white bar as nitrogen deficiency condition and gray bar as salt stress condition). Data are means ± standard deviation of three independent experiments.

4.2 Cloning and overexpression of *ACP* gene from *S. elongatus* PCC 7942

4.2.1 Cloning and expression of *ACP* from *S. elongatus* PCC 7942

To generate expressing plasmid, *ACP* together with its native promoter was amplified from genomic DNA of *S. elongatus* PCC 7942 by using specific primers as described in Materials and Methods. PCR products approximately 2.3 kb were sub-cloned into pGEM-T Easy vector. A recombinant plasmid harbouring *ACP* gene was confirmed by digestion with *Bam*HI and *Xho*I. To construct *ACP* with its native promoter in shuttle vector, the pUC303 was use as expression vector, DNA fragments covering *ACP* and its native promoter from cloning vector were prepared by digestion with *Bam*HI and *Xho*I from pGEM-T Easy vector. Then, the fragment was ligated into corresponding restriction sites of pUC303 expressing vector. To confirm the insertion, restriction enzyme analysis was performed by *Bam*HI and *Xho*I digestion. Electrophoresis result showed the inserted DNA fragment of *ACP* and its native promoter size approximately 2.3 kb after double digestion (Figure 20). The correct generated plasmid was transferred to *S. elongatus* PCC 7942 cells for overexpression.

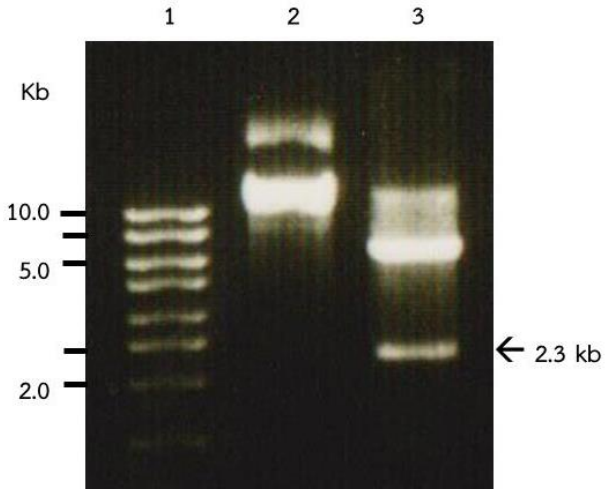

Figure 20: Restriction enzyme analysis of *ACP* with its native promoter. ACP7942/pUC303 plasmids were extracted from E. coli DH5α cells followed by double digestion of BamHI and XhoI. DNA fragments were seperated on 1.0 % (w/v) agarose gel with SYBR safe DNA gel staining for electrophoresis. Lane 1: DNA ladder, lane 2: non-digestion of ACP7942/pUC303, and lane 3: double digestion of ACP7942/pUC303 with *Bam*HI and *Xho*I.

4.2.2 Transformation of *ACP* into *S. elongatus* PCC 7942

To overexpress *ACP* in a wild-type strain *S. elongatus* PCC 7942, natural transformation was performed as described in Materials and Methods. After streptomycin addition, only candidate transformants could grow on selective BG11 plates (50 μg/ml of streptomycin). The single colony receiving pUC303 or recombinant plasmids (*ACP7942*/pUC303) would also appear on selective BG11 plates after growing for 3 weeks (Figure 21). For checking generated plasmid transformants, candidate clones were re-streaked on selective media. Then, colony PCR analysis was performed by using specific primers for *ACP* gene. The electrophoresis result shows in Figure 22. The overexpressing cells which obtained *ACP* recombinant plasmid (*ACP7942*/pUC303), had stronger band intensity of PCR products approximately 2.0 to 3.0 folds (as shown in lane 9 to 17) when compared with wild-type strain or control cells which *ACP* had only native expression. In

addition, we also detected PCR product of *streptomycin resistant* gene. All transformants receiving pUC303 or recombinant plasmid (*ACP7942*/pUC303) had *streptomycin resistant* band signals (data not shown).

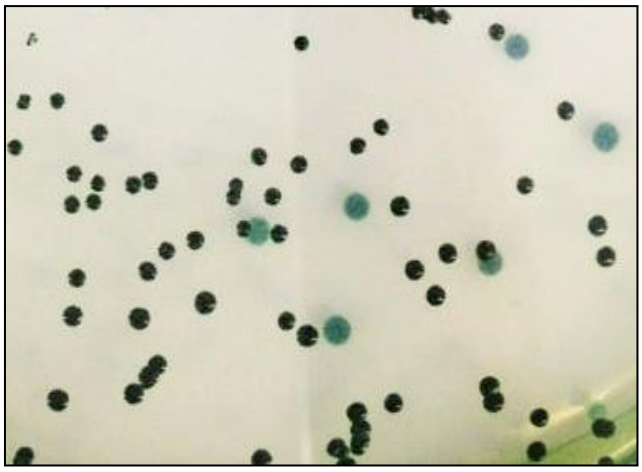

Figure 21: Candidate transformants harbouring *ACP7942*/pUC303 on BG11 plate supplemented with streptomycin (50μg/ml). *S. elongatus* PCC 7942 cells were obtained exogenous plasmids via natural transformation. Transformants were recovered on BG11 plate for 5 days then these transformants were selected by streptomycin addition to final concentration 50μg/ml and additionally cultured for 21 days.

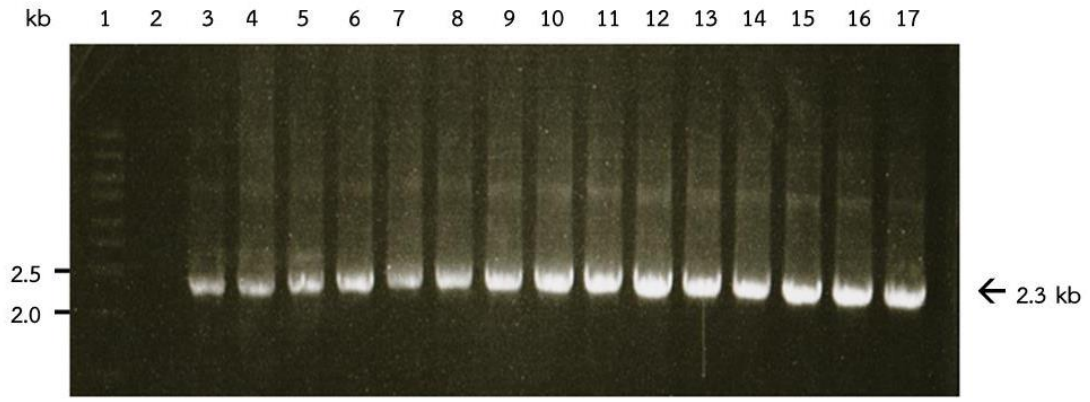

Figure 22: Colony PCR analysis of *ACP* with its native promoter amplification in *S. elongatus* PCC 7942 overexpressing cells. The PCR products were analyzed by electrophoresis using 1.0 % (w/v) agarose gel with SYBR safe DNA gel staining. The intensity of PCR product bands was carried out using Gel Doc EZ Imager program lane 1: DNA ladder, lane 2: negative control (no template DNA), lane 3: empty vector pUC303 (control cells), lane 4: wild-type strain cells, lane 5 to 17: candidate transformants of *ACP7942*/pUC303.

4.2.3 Lipid profile analysis

Lipid profile analysis was conducted in *S. elongatus PCC 7942* overexpressing cells. For this, *S. elongatus PCC 7942* control cells (harbouring pUC303 vector) and overexpressing cells (harbouring *ACP7942*/pUC303) were grown under two conditions such as normal (BG11 medium) and salt stress (BG11 medium containing 0.3 M of NaCl) conditions as described in 3.8.1. After 14 days of culturing, cyanobacterial cells were harvested by centrifugation. Then, intracellular fatty acids were extracted and esterificated as described in Materials and Methods. FAMEs were extracted by hexane containing 0.01 % BHT. After processing, extracts were analyzed by gas chromatography with a flame ionization detector and using helium as carrier gas.

Total fatty acid profiles of control and overexpressing cells were shown in Figure 23 and Table 3-4 the profile of esterified fatty acids showed some differences between control and overexpressing cells. In both normal and salt stress conditions,

control and overexpressing cells found several kinds of unsaturated and saturated fatty acids between C10 to C20. In addition, Palmitic acid (C16:0) and Palmitoleic acid (C16:1) were the majority of these fatty acids. In normal condition (Figure 23 A), amount of Palmitic acid and Palmitoleic acid in the overexpressing cells were higher than control cells. On the other hand, Oleic acid (C18:1) decreased in the overexpressing cells. Interestingly, total fatty acid content of the overexpressing cells was higher than control ones approximately 3.7 folds (Figure 24). In contrast, under salt-stress cultural condition (Figure 23 B), amount of Palmitic acid and Palmitoleic acid in the overexpressing cells were lower than control cells while Stearic acid (C18:0) and Oleic acid were higher than control cells. However, the total fatty acid content of the overexpressing cells had no difference when compared with control one (Figure 24). These data indicated that the overexpression of *ACP* in *S. elongatus* PCC 7942 could modulate fatty acid compositions under normal culture condition.

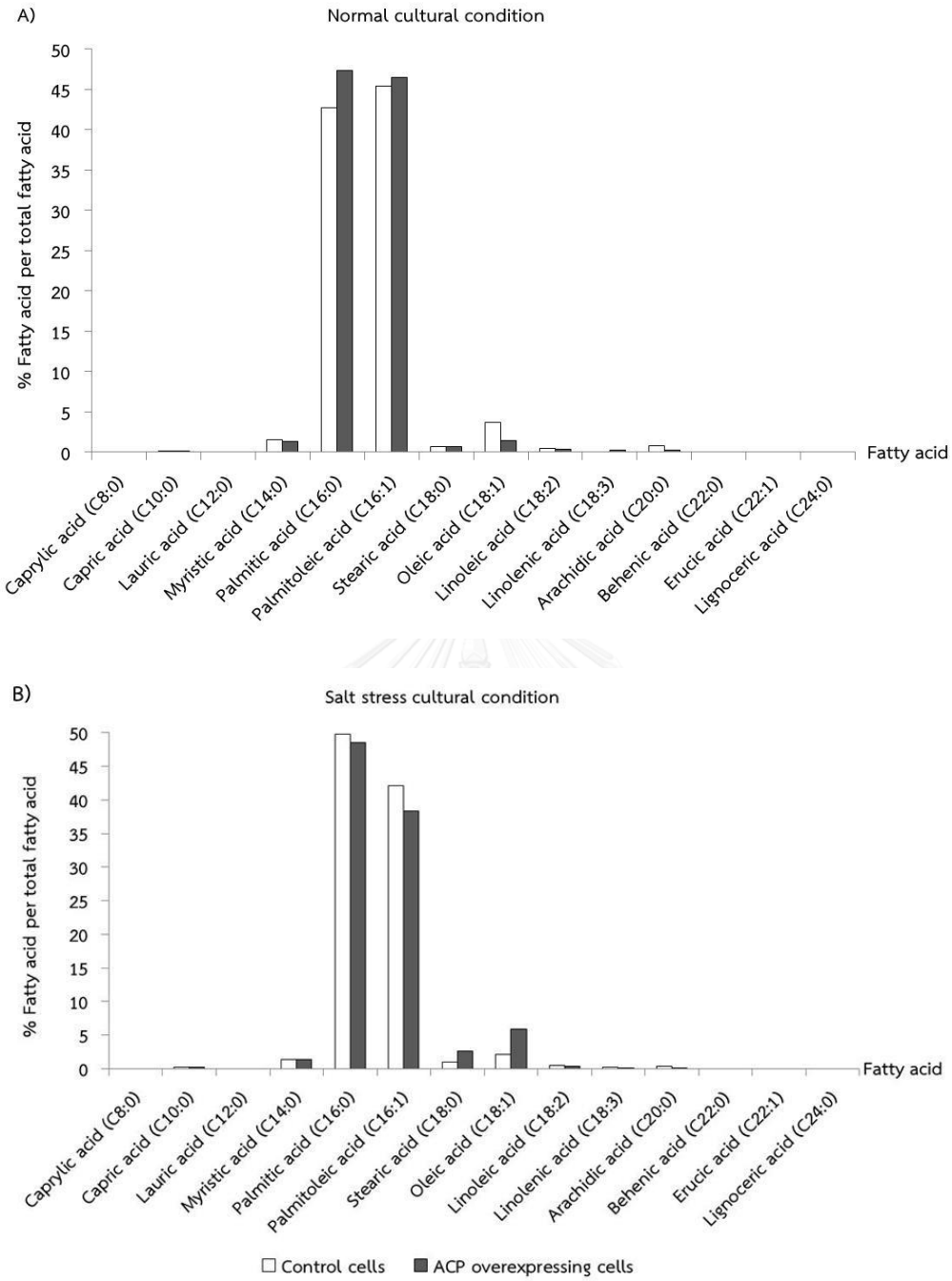

Figure 23: Intracellular fatty acid profiles of control and *ACP* overexpressing cells were grown under normal (A) and salt stress (B) conditions for 14 days in the present of 50 µg/ml of streptomycin. After harvesting the cells, intracellular fatty acids were extracted and esterificated into FAMEs by methanol-hydrochloric 95:5 (v/v). FAMEs were analyzed by gas chromatography. Percent of the total FAME, gray bars: fatty acids from expressing cells, and white bars: fatty acids from control cells.

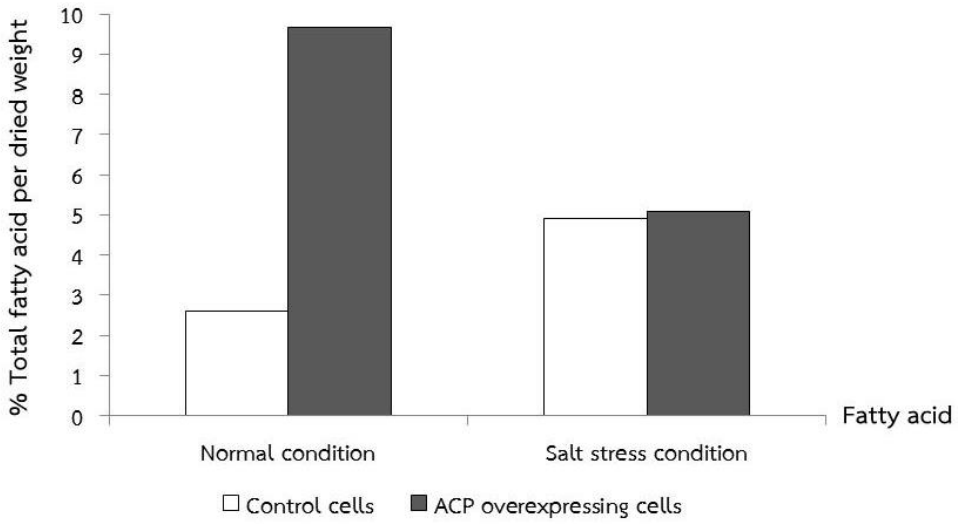

Figure 24: Comparison of total fatty acid per dried weight (%) in control and *ACP* overexpressing cells.

Table 3: Total fatty acid methyl ester (%) of control and *ACP* overexpressing cells under normal condition.

Fatty acid	% Fatty acid per total fatty acid	
	Control cells (WT)	*ACP* overexpressing cells (OX)
Caprylic acid (C8:0)	0.00	0.00
Capric acid (C10:0)	0.14	0.18
Lauric acid (C12:0)	0.00	0.00
Myristic acid (C14:0)	1.49	1.32
Palmitic acid (C16:0)	42.75	47.35
Palmitoleic acid (C16:1)	45.37	46.48
Stearic acid (C18:0)	0.72	0.65
Oleic acid (C18:1)	3.7	1.39
Linoleic acid (C18:2)	0.48	0.32
Linolenic acid (C18:3)	0.00	0.24
Arachidic acid (C20:0)	0.75	0.22
Behenic acid (C22:0)	0.00	0.00
Erucic acid (C22:1)	0.00	0.00
Lignoceric acid (C24:0)	0.00	0.00
% Total fatty acid per dried weight	2.61	9.67

Table 4: Total fatty acid methyl ester (%) of control and *ACP* overexpressing cells under salt stress condition.

Fatty acid	% Fatty acid per total fatty acid	
	Control cells (WT)	*ACP* overexpressing cells (OX)
Caprylic acid (C8:0)	0	0
Capric acid (C10:0)	0.18	0.19
Lauric acid (C12:0)	0	0
Myristic acid (C14:0)	1.34	1.4
Palmitic acid (C16:0)	49.79	48.57
Palmitoleic acid (C16:1)	42.1	38.4
Stearic acid (C18:0)	0.99	2.64
Oleic acid (C18:1)	2.08	5.92
Linoleic acid (C18:2)	0.55	0.36
Linolenic acid (C18:3)	0.27	0.16
Arachidic acid (C20:0)	0.36	0.17
Behenic acid (C22:0)	0	0
Erucic acid (C22:1)	0	0
Lignoceric acid (C24:0)	0	0
% Total fatty acid per dried weight	4.90	5.08

CHAPTER V
DISCUSSION

Due to continual decreasing of petroleum fuel, various kinds of biofuel resources have been developed to overcome the near world energy shortage crisis. Microalgae are the potential biofuel resources because of their unique metabolisms which can be developed to promote biofuel production (Hu *et al.*, 2008, La Russa *et al.*, 2012). Metabolic engineering is rapidly gained more attention to enhance biofuel production from microalgae. Lipid metabolism related genes are of particular interest. There are three main parts in microalgal lipid metabolism such as LD formation, free fatty acid synthesis, and hydrocarbon synthesis. In this study, two putative genes involved in lipid metabolism were cloned, expressed, and functionally analyzed. The first gene is *caleosin* from green alga *C. vulgaris* TISTR 8580. It encodes LD protein. The second gene is *ACP* from cyanobacterium *S. elongatus* PCC 7942. It encodes acyl carrier protein synthetase.

Amino acid sequence analysis of *Chlorella* caleosin reveals several signature domains which have also reported in other caleosin proteins (Figure 4.1). *Chlorella* caleosin has the putative calcium-binding EF-hand and proline-knot domains which are similar to fungi and plant caleosin proteins (Hanano *et al.*, 2006, Blee *et al.*, 2012). However, it has shown that *Chlorella* caleosin has a single calcium-binding EF-hand domain whereas AtClo1, *Arabidopsis* caleosin proteins show two calcium-binding EF-hand domains (Hanano *et al.*, 2006). In *Arabidopsis thaliana,* seven putative genes for caleosin have been reported, but only three genes (*AtClo1*, 2, and *4*) were functionally characterized. The *Arabidopsis* caleosin AtClo1, has a calcium-dependent heme oxygenase activity by two conserved ferric-binding histidine residues (Hanano *et al.*, 2006). The conserved histidine residues also were found in *Chlorella* caleosin (Figure 4.1). It should be noted that *Chlorella* caleosin isolated from this study has extra insertion of amino acids at C-terminus (Figure 4.1). This part is absent in other previously reported caleosins.

For physicochemical properties, *Chlorella* caleosin protein has theoretical pI of 8.54 and molecular mass of 31 kDa. Theoretical pI of *Chlorella* caleosin is unique because other caleosins have mainly theoretical pI ranging from 5-9. In contrast, theoretical molecular masses of caleosins are diverse which in the ranging of 21-34 kDa (Table 2). Topological model of *Chlorella* caleosin comprises of a single hydrophobic part at the center (Figure 10), thus *Chlorella* caleosin protein was classified into class I group of caleosin according to hydropathy plot. It has been shown that hydrophobic part of class II group is located at the N-terminus (Hanano *et al.*, 2006). Phylogenetic tree suggests the evolutionary relationship of *Chlorella* caleosin protein with other caleosin proteins. *Chlorella* caleosin protein is more similar to fungi (Q7S2T2) and plant (At1g23240) caleosin proteins than algal caleosin proteins (Figure 4.3). Correspondingly, plant caleosin (At1g23240) was also classified into class I group of caleosin by hydropathy classification (Hanano *et al.*, 2006).

For recombinant caleosin protein expression, we have successfully expressed recombinant caleosin protein from *C. vulgaris* TISTR 8580 in *E. coil* strain BL21 under cspA promoter. By SDS-PAGE analysis, the molecular mass was observed as 32 kDa which in good agreement with the theoretical molecular mass (Figure 12). *Chlorella* caleosin protein was constructed to fused-in-frame with 6X-His tag at the N-terminus; thereby, it could be purified by Ni-affinity chromatography (Figure 13-4.6). By the driven of cspA promoter, *Chlorella* caleosin could express in soluble form, although it could also observe some amounts as insoluble form (data not shown). In many cases, caleosin proteins found as insoluble proteins. There is probably due to its hydrophobicity and membrane bound property therefore fusion tag proteins were needed to assist folding and solubilizing. For example, caleosin-related protein (RD20) from *A. thaliana* was found to be able to express together with glutatione S-transferase (GST) (Takahashi *et al.*, 2000).

Functional characterization indicated that *Chlorella* caleosin has no calcium binding property, but having peroxygenase activity. It is a hemoprotein. As far as we know, this study is the first case of functional analysis for microalgal caleosin protein.

Firstly, calcium binding activity was carried out by the mobility shift on polyacrylamide gel. In case of calcium binding protein, the binding of calcium will interrupt protein mobility on polyacrylamide gel resulting in mobility shift of protein-calcium binding complex. In the present of EGTA, a chelating agent which can bind with calcium ion competitively to protein resulting in no mobility shift or no protein-calcium binding complex. Although *Chlorella* caleosin protein contained putative calcium-binding EF-hand domain, the result of calcium binding showed no mobility shift on polyacrylamide gel (Figure 15). There are two plausible reasons. Firstly, N-terminus fusion of the protein might be the reason. From caleosin protein structure, calcium-binding EF-hand domain was found at the N-terminus which fused-in-frame with 6X-His tag. This might affect calcium-binding property (Chapman *et al.*, 2012). Secondly, at least two EF-hand motifs maybe required for calcium-binding. For instance, Calbindin D_{9k} protein containing a single N-terminal EF-hand prefers to dimerize in the calcium binding state (Julenius *et al.*, 2002).

Peroxygenase is a versatile oxygenase enzyme with strictly hydroperoxide-dependency. Several reactions can occur by peroxygenase depend on kind of substrates (Hanano *et al.*, 2006). Sulfoxidation, hydroxylation, and epoxidation are occurred when xenobiotics, aromatics, and unsaturated fatty acids are used as substrates, respectively. Some caleosin proteins have unique substrate specificities, such as aniline for hydroxylation is the substrate preference of *Arabidopsis* caleosin AtClo1 protein while AtClo4 prefers oleic acid as a substrate for epoxidation (Blee *et al.*, 2012). Here, peroxygenase activity of recombinant caleosin protein was examined using aniline and oleic acid as a substrate for hydroxylation and epoxidation (data not shown), respectively. In this study, only hydroxylation could occur in recombinant caleosin protein (Figure 16). For hemoprotein characterization (Figure 17), recombinant caleosin protein performed as hemoprotein similar to *Arabidopsis* caleosin AtClo1 (Hanano *et al.*, 2006). Physiological studies by Nile red staining and Semiquantitative RT-PCR of *caleosin* gene have been examined in *C. vulgaris* TISTR 8580 under nitrogen deficiency, salt stress, and sodium acetate stress conditions, respectively (Figure 18-19). All stress conditions induced LD accumulation. For

nitrogen deficiency, this condition is a common condition to induce LD formation because of imbalance of carbon and nitrogen ratio (Pasaribu *et al.*, 2014). Interestingly, salt stress condition has no report in LD accumulation. Salt stress condition is interesting because most organisms will adapt themselves to thrive and survive under high salt condition by various mechanisms. For example, some algae could accumulate trehalose and sucrose as osmolytes under high-salt condition (Bremauntz, 2011). For sodium acetate stress, this condition could greatly promote both LD formation and growth of cells in *C. vulgaris* TISTR 8580. In previous study, LD formation was limited by acetate availability in starchless mutant of *Chlamydomonas reinhardtii* because acetate is a precursor of acetyl-CoA production which is requited for the first step of LD assembly (Ramanan *et al.*, 2013). Although sodium acetate stress condition could greatly promote both LD formation and growth of cells, the culture of *C. vulgaris* TISTR 8580 in this condition had some technical problem. In sodium acetate stress culture, *Chlorella* cells were slime sediments after cells harvesting. Thus, only nitrogen deficiency and salt stress conditions were used in further semiquantitative RT-PCR of *caleosin* gene.

For fatty acid synthesis approach, the overexpression of *ACP* has been reported in cyanobacteria under the driven of strong promoter but these systems did not well successfully for expression (Kaczmarzyk & Fulda, 2010, Ruffing & Jones, 2012). Here, overexpression of *ACP* under native promoter in cyanobacterium *S. elongatus* PCC 7942 was performed. Our results showed that *ACP* with its native promoter was successfully constructed and overexpressed in *S. elongatus* PCC 7942. The overexpressors were confirmed by the ability to grow on BG11 supplemented with streptomycin and colony PCR analysis with specific primers of *ACP* and streptomycin genes (data not shown). For lipid profile analysis, fatty acid compositions were slightly changed when compared with control ones under both conditions (Figure 23). We found total fatty acid contents of the overexpressing cells were higher than control one approximately 3.7- fold under normal (Figure 24). Lipid profile results suggest that normal condition promoted lipid accumulation more than salt stress condition. Palmitic acid and Palmitoleic acid are dominant fatty acids in

overexpressing cells (Figure 23 and Table 3-4) that corresponded to Kaczmarzyk and Fulda (2010) that C16 fatty acid was specific substrate for acyltransferases in prokaryotic organisms.

To summarize, this study reports that *caleosin* gene is successfully isolated from *C. vulgaris* TISTR 8580 by RACE-method. Recombinant caleosin protein can express in *E. coli* strain BL21 and purify by affinity chromatography. Functional characterization suggests that *Chlorella* caleosin exhibits peroxygenase activity and hemoprotein but no calcium binding activity. Physiological study suggests that LD formation can be well induced under nitrogen deficiency and salt stress conditions. For ACP, *ACP* is successfully isolated and overexpressed in *S. elongatus* PCC 7942 with its native promoter under normal induced condition. Lipid profiles analysis indicates that fatty acid content is modulated in the overexpressing cells.

CHAPTER VI

CONCLUSION

I) Full length of *caleosin* gene encoding lipid droplet protein was successfully isolated from *C. vulgaris* TISTR 8580 by RACE-method.

II) Caleosin protein was successfully expressed in *E. coli* strain BL21.

III) Functional characterization of *Chlorella* caleosin reveals no calcium binding property but it has peroxygenase and hemoprotein.

IV) *Caleosin* gene was up-regulated by salt-stress and nitrogen deficiency conditions.

V) *ACP* gene from *S. elongatus* PCC 7942 was cloned and overexpressed under the driven of native promoter.

VI) Palmitic (C 16:0) and palmitoleic (C 16:1) acids are major fatty acids found in the overexpressor.

VII) Total fatty acid of the overexpressor was higher than control approximately 3.7-fold under normal condition but no change under salt-stress condition.

REFERENCES

Artimo P, Jonnalagedda M, Arnold K, *et al.* (2012) ExPASy: SIB bioinformatics resource portal. *Nucleic acids research* **40**: W597-603.

Blee E, Flenet M, Boachon B & Fauconnier ML (2012) A non-canonical caleosin from Arabidopsis efficiently epoxidizes physiological unsaturated fatty acids with complete stereoselectivity. *The FEBS journal* **279**: 3981-3995.

Bradford MM (1976) A rapid and sensitive method for the quantitation of microgram quantities of protein utilizing the principle of protein-dye binding. *Analytical biochemistry* **72**: 248-254.

Bremauntz MdP (2011) Trehalose and Sucrose Osmolytes Accumulated by Algae as Potential Raw Material for Bioethanol. *Natural Resources* **02**: 173-179.

Chapman KD, Dyer JM & Mullen RT (2012) Biogenesis and functions of lipid droplets in plants: Thematic Review Series: Lipid Droplet Synthesis and Metabolism: from Yeast to Man. *Journal of lipid research* **53**: 215-226.

Fernandes BD, Dragone GM, Teixeira JA & Vicente AA (2010) Light regime characterization in an airlift photobioreactor for production of microalgae with high starch content. *Applied biochemistry and biotechnology* **161**: 218-226.

Hanano A, Burcklen M, Flenet M, Ivancich A, Louwagie M, Garin J & Blee E (2006) Plant seed peroxygenase is an original heme-oxygenase with an EF-hand calcium binding motif. *The Journal of biological chemistry* **281**: 33140-33151.

Hill J, Nelson E, Tilman D, Polasky S & Tiffany D (2006) Environmental, economic, and energetic costs and benefits of biodiesel and ethanol biofuels. *Proceedings of the National Academy of Sciences of the United States of America* **103**: 11206-11210.

Hu Q, Sommerfeld M, Jarvis E, Ghirardi M, Posewitz M, Seibert M & Darzins A (2008) Microalgal triacylglycerols as feedstocks for biofuel production: perspectives

and advances. *The Plant journal : for cell and molecular biology* **54**: 621-639.

Huang G, Chen F, Wei D, Zhang X & Chen G (2010) Biodiesel production by microalgal biotechnology. *Applied Energy* **87**: 38-46.

Julenius K, Robblee J, Thulin E, Finn BE, Fairman R & Linse S (2002) Coupling of ligand binding and dimerization of helix-loop-helix peptides: spectroscopic and sedimentation analyses of calbindin D_{9k} EF-hands. *Proteins* **47**: 323-333.

Kaczmarzyk D & Fulda M (2010) Fatty acid activation in cyanobacteria mediated by acyl-acyl carrier protein synthetase enables fatty acid recycling. *Plant physiology* **152**: 1598-1610.

Kuhlemeier CJ & van Arkel GA (1987) Host-vector systems for gene cloning in cyanobacteria. *Methods in enzymology* **153**: 199-215.

La Russa M, Bogen C, Uhmeyer A, Doebbe A, Filippone E, Kruse O & Mussgnug JH (2012) Functional analysis of three type-2 DGAT homologue genes for triacylglycerol production in the green microalga *Chlamydomonas reinhardtii*. *Journal of biotechnology* **162**: 13-20.

Laemmli UK (1970) Cleavage of structural proteins during the assembly of the head of bacteriophage T4. *Nature* **227**: 680-685.

Li Y (2008) Articles: biocatalysts and bioreactor design. *Biotechnol Prog* **24**: 815-820.

Lin F, Das D, Lin XN & Marsh EN (2013) Aldehyde-forming fatty acyl-CoA reductase from cyanobacteria: expression, purification and characterization of the recombinant enzyme. *The FEBS journal* **280**: 4773-4781.

Lin IP, Jiang PL, Chen CS & Tzen JT (2012) A unique caleosin serving as the major integral protein in oil bodies isolated from *Chlorella* sp. cells cultured with limited nitrogen. *Plant physiology and biochemistry : PPB / Societe francaise de physiologie vegetale* **61**: 80-87.

Liu A, Tan X, Yao L & Lu X (2013) Fatty alcohol production in engineered *E. coli* expressing Marinobacter fatty acyl-CoA reductases. *Applied microbiology and biotechnology* **97**: 7061-7071.

Liu Y, Zhang C, Shen X, Zhang X, Cichello S, Guan H & Liu P (2013) Microorganism lipid droplets and biofuel development. *BMB Reports* **46**: 575-581.

Mata TM, Martins AA & Caetano NS (2010) Microalgae for biodiesel production and other applications: A review. *Renewable and Sustainable Energy Reviews* **14**: 217-232.

Metzger P & Largeau C (2005) *Botryococcus braunii*: a rich source for hydrocarbons and related ether lipids. *Applied microbiology and biotechnology* **66**: 486-496.

Nguyen AV, Thomas-Hall SR, Malnoe A, Timmins M, Mussgnug JH, Rupprecht J, Kruse O, Hankamer B & Schenk PM (2008) Transcriptome for photobiological hydrogen production induced by sulfur deprivation in the green alga *Chlamydomonas reinhardtii*. *Eukaryotic cell* **7**: 1965-1979.

Nomura M, Ishitani M, Takabe T, Rai AK & Takabe T (1995) *Synechococcus* sp. PCC7942 Transformed with *Escherichia coli* bet Genes Produces Glycine Betaine from Choline and Acquires Resistance to Salt Stress. *Plant physiology* **107**: 703-708.

Pasaribu B, Lin IP, Chen CS, Lu CY & Jiang PL (2014) Nutrient limitation in *Auxenochlorella protothecoides* induces qualitative changes of fatty acid and expression of caleosin as a membrane protein associated with oil bodies. *Biotechnology letters* **36**: 175-180.

Patil V, Tran KQ & Giselrod HR (2008) Towards sustainable production of biofuels from microalgae. *International journal of molecular sciences* **9**: 1188-1195.

Peled E, Leu S, Zarka A, Weiss M, Pick U, Khozin-Goldberg I & Boussiba S (2011) Isolation of a novel oil globule protein from the green alga *Haematococcus pluvialis* (Chlorophyceae). *Lipids* **46**: 851-861.

Radakovits R, Jinkerson RE, Darzins A & Posewitz MC (2010) Genetic engineering of algae for enhanced biofuel production. *Eukaryotic cell* **9**: 486-501.

Ramanan R, Kim BH, Cho DH, Ko SR, Oh HM & Kim HS (2013) Lipid droplet synthesis is limited by acetate availability in starchless mutant of *Chlamydomonas reinhardtii*. *FEBS letters* **587**: 370-377.

Rippka R, Deruelles J, Waterbury JB, Herdman M & Stanier RY (1979) Generic assignments, strain histories and properties of pure cultures of cyanobacteria. *J Gen Microbiol* **111**: 1-61.

Ruffing AM & Jones HD (2012) Physiological effects of free fatty acid production in genetically engineered *Synechococcus elongatus* PCC 7942. *Biotechnology and bioengineering* **109**: 2190-2199.

Sambrook J, Fritsch EF & Maniatis T (1989) Molecular cloning. 2nd ed: A laboratory manual. Cold Spring Harbor Laboratory Press, New York.

Schenk PM, Thomas-Hall SR, Stephens E, Marx UC, Mussgnug JH, Posten C, Kruse O & Hankamer B (2008) Second generation biofuels: high-efficiency microalgae for biodiesel production. *BioEnergy Research* **1**: 20-43.

Schirmer A, Rude MA, Li X, Popova E & del Cardayre SB (2010) Microbial biosynthesis of alkanes. *Science* **329**: 559-562.

Scott SA, Davey MP, Dennis JS, Horst I, Howe CJ, Lea-Smith DJ & Smith AG (2010) Biodiesel from algae: challenges and prospects. *Current opinion in biotechnology* **21**: 277-286.

Stephens E, Ross IL, King Z, Mussgnug JH, Kruse O, Posten C, Borowitzka MA & Hankamer B (2010) An economic and technical evaluation of microalgal biofuels. *Nat Biotechnol* **28**: 126-128.

Takahashi S, Katagiri T, Yamaguchi-Shinozaki K & Shinozaki K (2000) An Arabidopsis gene encoding a Ca^{2+}-binding protein is induced by abscisic acid during dehydration. *Plant & cell physiology* **41**: 898-903.

the U.S. Energy Information Administration (EIA) (2012) The Annual Energy Outlook 2012.

Wagner M, Hoppe K, Czabany T, Heilmann M, Daum G, Feussner I & Fulda M (2010) Identification and characterization of an acyl-CoA:diacylglycerol acyltransferase 2 (DGAT2) gene from the microalga *O. tauri*. *Plant physiology and biochemistry : PPB / Societe francaise de physiologie vegetale* **48**: 407-416.

Yuasa K & Maeshima M (2000) Purification, properties, and molecular cloning of a novel $Ca^{(2+)}$-binding protein in radish vacuoles. *Plant physiology* **124**: 1069-1078.

APPENDICES

APPENDIX 1

LB medium

Composition per 1 liter

10 g	Bacto tryptone
5 g	Yeast extract
10 g	NaCl

Dissolve all compositions with 800 ml deionizaed water, adjust the pH to 7.0 with 6 M NaOH. Adjust volume of solution to 1 liter with deionizaed water. Autoclave at 121 °C, 15 lb/in2 for 15 min. For media containing agar add bactoagar 15 g per liter.

APPENDIX 2

BG11 medium

Trace element solution

H_3BO_3	2.8 g
$MnCl_2.4H_2O$	1.81 g
$ZnSO_4.7\ H_2O$	0.22 g
$CuSO_4.5\ H_2O$	0.079 g
$Co(NO_3)_2.6H_2O$	0.049 g

Dissolved all compositions with distilled water to 1 liter.

BG11 solution

$NaNO_3$	1.5 g
$K2PO_4$	40 mg
$MgSO_4.7H_2O$	75 mg
$CaCl_2.H_2O$	36 mg
Na_2CO_3	20 mg
EDTA*2Na	1 mg
Citric acid	6 mg
Ferric ammonium nitrate	6 mg
Trace element	1 ml

Dissolved all compositions with distilled water to 1 liter.

APPENDIX 3

Preparation for polyacrylamide gel electrophoresis

1. Stock reagents

30% Acrylamide, 0.8% bis acrylamide, 100 ml

Acrylamide	29.2 g
N, N´ methylene bis acrylamide	0.8 g

Adjust volume to 100 ml with distill water.

1.5 M Tris Cl pH 8.8

Tris (hydroxymethyl) aminomethane	18.17 g

Adjust pH to 8.8 and adjust volume to 100 ml with distill water.

2 M Tris Cl pH 8.8

Tris (hydroxymethyl) aminomethane	24.2 g

Adjust pH to 8.8 and adjust volume to 100 ml with distill water.

0.5 M Tris Cl pH 6.8

Tris (hydroxymethyl) aminomethane	6.06 g

Adjust pH to 8.8 and adjust volume to 100 ml with distill water.

1 M Tris Cl pH 6.8

Tris (hydroxymethyl) aminomethane	12.1 g

Adjust pH to 8.8 and adjust volume to 100 ml with distill water.

Solution B (SDS-PAGE)

2 M Tris Cl pH 8.8	75 ml
10% SDS	4 ml

Distill water 21 ml

Solution C (SDS-PAGE)

2 M Tris Cl pH 6.8	50 ml
10% SDS	4 ml
Distill water	46 ml

2. SDS-PAGE

10% separating gel

30% acrylamide solution	3.33 ml
Solution B	2.5 ml
Distill water	5.0 ml
10% Ammonium sulfate	50 µl
TEMED	10 µl

5% stacking gel

30% acrylamide solution	0.67 ml
Solution B	1.0 ml
Distilled water	2.3 ml
10% Ammonium sulfate	30 µl
TEMED	5.0 µl

Sample buffer

1M Tris Cl pH 6.8	0.6 ml
50% glycerol	5.0 ml
10% SDS	2.0 ml
2 mercaptoethanol	0.5 ml
1% bromphenol blue	1.0 ml
Distilled water	0.9 ml

4x of sample buffer is mixture sample to 1x. The mixture heated 5 min in boiling water before loading to the gel.

Electrophoresis buffer for 1 litre

Tris (hydroxymethyl) aminomethane	3.0 g
Glycine	14.4 g
SDS	1.0 g

Adjust volume to 1 litre with distilled water (pH 8.3).

APPENDIX 4

Buffer for western blotting

PBS buffer (Phosphate-buffer-saline)

Final concentration per 1 lite

10 mM sodium phosphate pH 7.4

150 mM NaCl

Blocking buffer

5% (w/v) skim milk and 0.01% Tween20 in 1x PBS buffer

Blotting transfer buffer

Final concentration per 1 liter

39 mM glycine

48 mM Tris base

0.037 % SDS

20 % methanol

APPENDIX 5

Standard protein

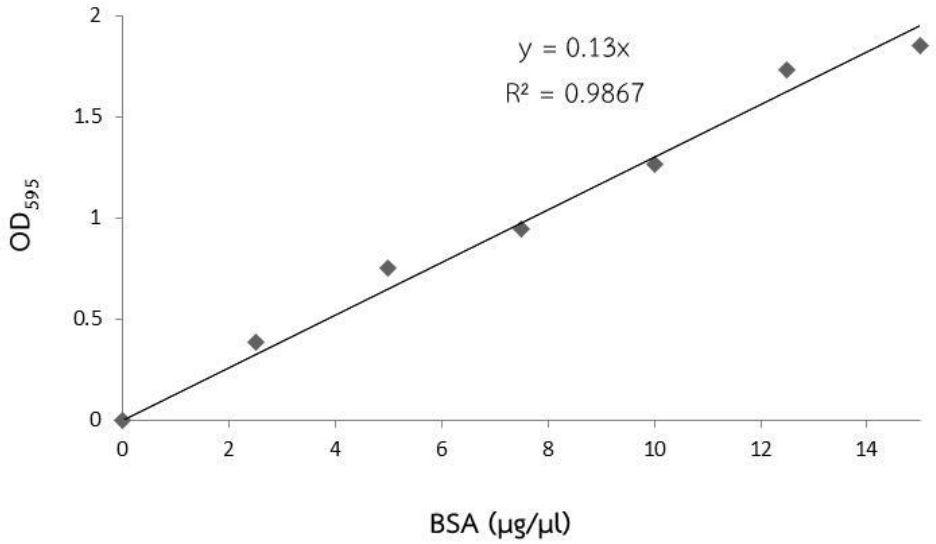

APPENDIX 6

Nile red solution

Nile red stock solution

Nile red 250 mg

Adjust volume to 1 milliliter with acetone and kept in a tightly sealed, lightproof container at 4 degrees.

Preparing the stain for use (100x dilution)

Final concentration per 1 milliliter

Nile red stock solution 10 µl

Adjust volume to 1 milliliter with 50mM Tris/Maleate. It is mixed using a magnetic stirrer. This solution can keep in a lightproof container for a few months at 4 degrees.

VITA

Miss Pairpilin Charuchinda was born on October 21, 1989 in Kanchanaburi, Thailand. She graduated from Department of Microbiology, Faculty of Science, Chulalongkorn University in 2012 with a Bachelor degree of Science (Microbiology). Recently, she has pursued her Master degree of Program in Biotechnology, Faculty of Science, Chulalongkorn University and then some parts of this work published in the 26th annual meeting of the Thai society for biotechnology and international conference in 2014.